Maria Masip Sanchis

Optimization and standardisation of RT-qPCR methodology to detect B.1.1.7 and B.1.351 variants of SARS-CoV-2 in wastewater

Final degree project

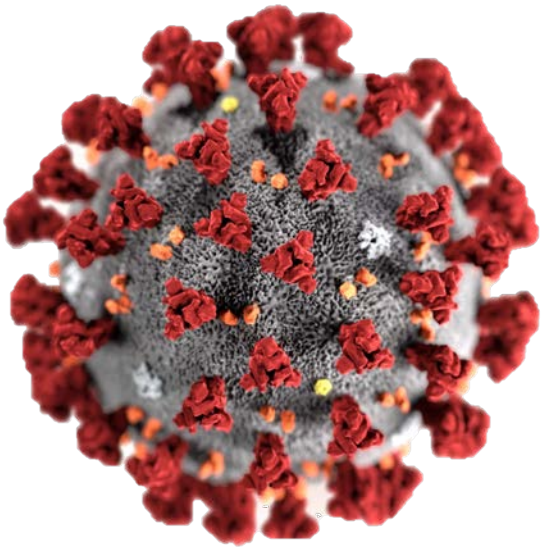

Professional tutor: Dra. Ester Méndez Belinchón, SARS-CoV-2 Department Manager

Academic tutor: Dr. Pere Puigbo Àvalos, Department of Biochemistry and Biotechnology

Biotechnology and Biochemistry and molecular biology Double Degree

Universitat Rovira i Virgili
Tarragona
2021

UNIVERSITAT ROVIRA i VIRGILI

global omnium

This project is based on the results obtained in the external internship carried out at Gamaser under the tutelage of Dra. Ester Mendez Belinchón.

TABLE OF CONTENTS

1. ABSTRACT 3
2. INTRODUCTION 4
2.1. Variants of SARS-CoV-2 8
2.2. RT-qPCR 11
2.3. RT-qPCR in wastewater samples 14
3. HYPOTHESIS AND OBJECTIVES 15
4. METHODS 15
4.1. Concentration 16
4.2. Extraction 17
4.3. RT-qPCR 18
4.3.1. SARS-CoV-2 B.1.1.7 variant 18
4.3.2. SARS-CoV-2 B.1.351 variant 20
5. RESULTS 22
5.1. Optimization of the methods 22
5.1.1. SARS-CoV-2 B.1.1.7 variant 22
5.1.2. SARS-CoV-2 B.1.351 variant 26
5.2. Calibration of the methods 28
5.3. Results interpretation 32
5.4. Monitoring of SARS-CoV-2 variants in wastewater samples 35
6. DISCUSSION 37
6.1. Optimization of the methods 37
6.1.1. SARS-CoV-2 B.1.1.7 variant 37
6.1.2. SARS-CoV-2 B.1.351 variant 40
6.2. Calibration of the methods 40
6.3. Monitoring of SARS-CoV-2 variants in wastewater samples 41
7. CONCLUSION 44
8. BIBLIOGRAPHY 45
9. ANNEX 49

1. ABSTRACT

SARS-CoV-2 pandemic is considered one of the most important threats to humanity in the last centuries. SARS-CoV-2 is the virus responsible for alteration the population's normal way of life and, after a year of its emergence, the economic, social and health consequences were still evident. This virus is highly transmissible and is responsible for a huge number of deaths worldwide. The scientific community have been united all its efforts to pandemic ending, whereas the outbreak of new SARS-CoV-2 variants threatens to shatter all the progress made. The increased transmissibility and vaccine resistance properties of new variants are of great concern. This highlights the need for variants spread monitoring. Since the beginning of the pandemic, analysing wastewater by quantitative reverse transcription polymerase chain reaction (RT-qPCR) have elucidated its great potential. It is an early warning system that allowed a close tracking of the virus spreading, as positive and asymptomatic cases are possible to be detected. In this project, methodologies to detect SARS-CoV-2 B.1.1.7 and B.1.351 variants in wastewater are presented, which allowed us to track these variants in the region of Valencia between 31st March to 23rd April 2021.

2. INTRODUCTION

Severe acute respiratory syndrome coronavirus 2 (SARS-CoV-2) had firstly emerged in December 2019 in Wuhan (China) and since then the population's life has changed drastically. It is the responsible agent for the coronavirus disease 2019 (COVID-19) (1). On 30th January, the World Health Organization (WHO) declared the SARS-CoV-2 outbreak as a Public Health Emergency of International Concern (PHEIC) and many countries developed guidelines to control the spread of the virus, such as complete home confinement, suspension of academic activities, restriction of travel and trade, closure of the catering industry, etc. SARS-CoV-2 is responsible for millions of deaths worldwide, as well as alteration of healthcare service attendance, mental and physical health problems and severe economic consequences (2). Other coronaviruses have posed a threat to human health before SARS-CoV-2, such as the outbreak of severe acute respiratory syndrome coronavirus (SARS-CoV) and Middle East respiratory syndrome coronavirus (MERS-CoV) in 2002 and 2012, respectively. However, SARS-CoV-2 was the only one capable of triggering a pandemic due to a faster capacity of infection. These three coronaviruses belong to the family *Coronaviridae* and they are characterized by single-stranded positive-sense RNA genome (+ssRNA) (3).

The +ssRNA genome of SARS-CoV-2 is composed by 5' untranslated region (UTR), 15 open reading frames (ORFs), structural genes, accessory genes placed between the structural genes, and 3' UTR (Figure 1). The main ORF are ORF1a and ORF1b, which are translated into polyproteins. The structural genes encode for four proteins: spike (S), envelope (E), membrane (M) and nucleocapsid (N) (Table 1), which are essential for virus life cycle (3).

Figure 1. Genome architecture of SARS-CoV-2 mRNA. It has a leader sequence (LS), poly-A tail at 3' end, and 5' and 3' UTR. It consists of ORF1a, ORF1b, Spike (S), ORF3a, Envelope (E), Membrane (M), ORF6, ORF7a, ORF7b, ORF8, Nucleocapsid (N), and ORF10. Extracted and modified from Naqvi *et al.* (4).

Table 1. Description of four structural genes encoded in SARS-CoV-2 genome. Extracted from Al-Qaaneh *et al.* (5) and Arya *et al*. (6).

Gene	Base length	Protein	Protein function	Protein structure
S	3822	Spike protein	Binding to cell receptor and mediate virus-cell fusion	Composed by two subunits: S1, which acts as a surface antigen required for host interaction, and S2, which mediates cell-virus membrane fusion
E	228	Envelope protein	Assembly and release of virions, and pathogenesis contribution	Composed by two domains: hydrophobic transmembrane domain and charged cytoplasmic tail
M	669	Membrane protein	Central role in virus assembly and pathogenesis contribution	Composed by three transmembrane domains
N	1260	Nucleocapsid protein	Contribution in viral replication, transcription, virion structure, and viral assembly	Composed by three conserved domains important in protein structure and function

SARS-CoV-2 structure is characterized by a spherical envelope with different S proteins located as a projections (Figure 2). S gene is the most variable sequence of coronaviruses, whereas E, M and N genes are highly conserved between coronaviruses. Concretely, the most variable region of S protein is the receptor-binding domain (RBD), which recognises selectively the host receptor human angiotensin-converting enzyme 2 (ACE2) (7). This host receptor is present in many organs, such as lungs, arteries, kidneys, heart and intestines, indicating a multifactorial capacity of infection of SARS-CoV-2 (7). Furthermore, elevated levels of ACE2 were detected in epithelial cells of oral cavity, which indicates a high susceptibility to infection through the oral cavity (8) (Figure 3).

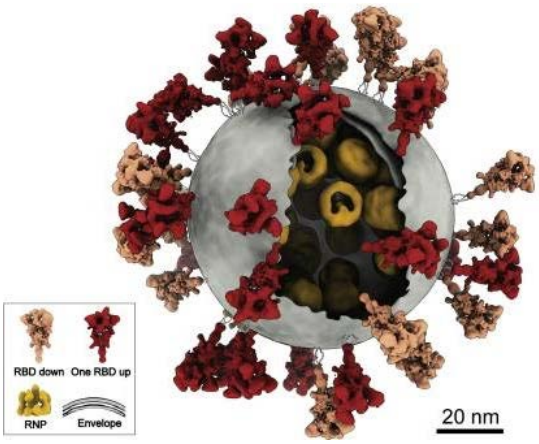

Figure 2. Representation of SARS-CoV-2 structure. Extracted and adapted from Yao *et al.* (9).

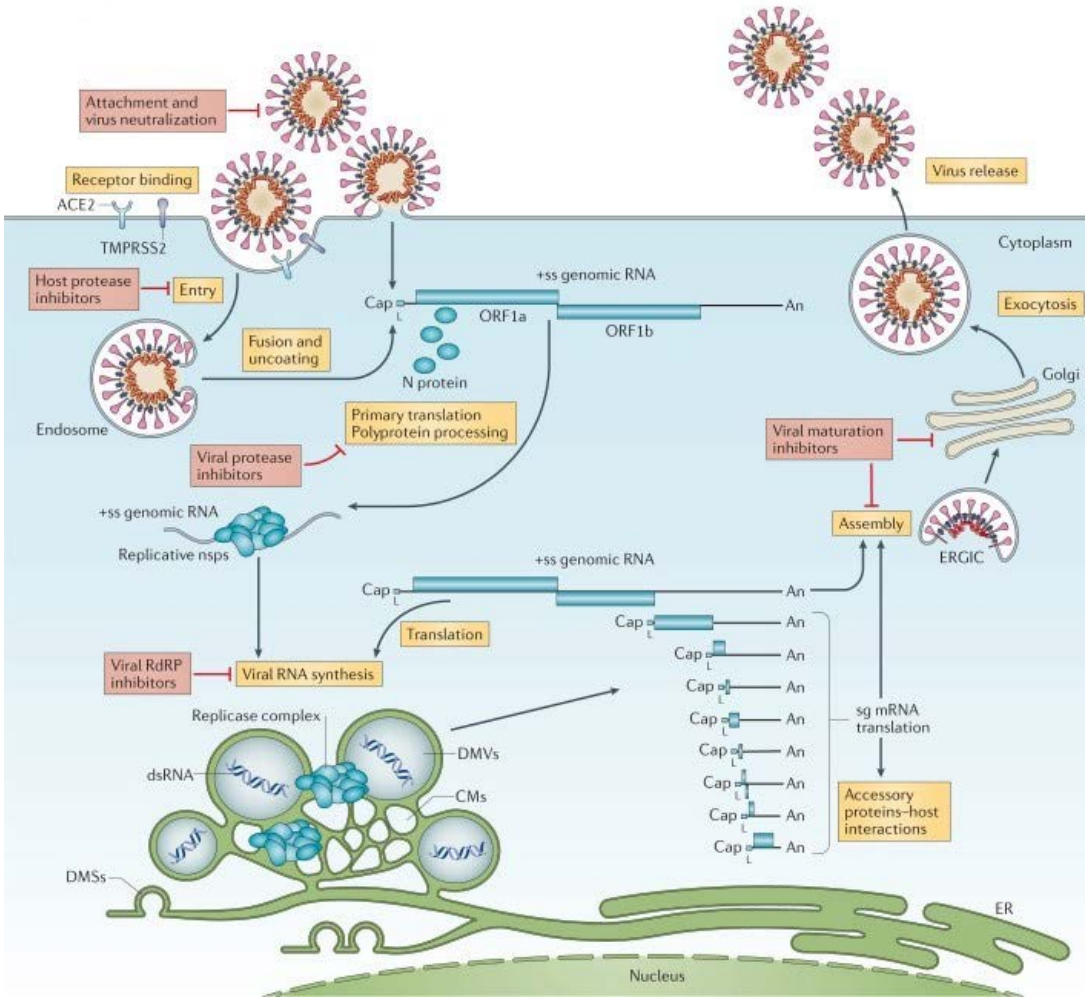

Figure 3. SARS-CoV-2 host cell infection. S1 domain of S protein interacts with the host receptor ACE2 and S2 domain mediates membrane fusion between host cell and the virus. The hosts factors interact with the viral RNA to synthesize new chains: the negative-sense RNA is synthesized and is used as a template to produce positive-sense RNA, which is used for new virions package and for translation to polyproteins, both using the host machinery. Once translated, the polyproteins are submitted to modifications post-translation to generate non-structural proteins (nsps) and these nsps create a replication transcription complex (RTC), which provides a protective microenvironment for viral RNA replication and transcription. The mRNA generated is translated into structural and accessory proteins. Viral RNA genome and proteins are assembled to generate virions in the Endoplasmic Reticulum (ER) and Golgi Apparatus (GA). Finally, the endosome containing the virion is released from the cell through endosome-membrane fusion (7). Extracted and modified from V'kovski *et al.* (10).

SARS-CoV-2 dominant route of transmission person-to-person is through respiratory droplets and aerosols (11). It was determined an incubation period of SARS-CoV-2 of 1-14 days, being 3rd to 7th days the most contagious. Moreover, some infected people can be asymptomatic and, although transmission rate is lower than symptomatic people, they can infect other people and be an important source of virus propagation (12). The main clinical symptoms are similar to influenza's symptoms, such as sore

throat, fever, cough, fatigue, shortness of breath and headache. In addition, gastrointestinal and neurological symptoms have also been identified in some patients. Most of the people develop mild symptoms, whereas people with co-morbidities (diabetes, hypertension, pulmonary disease, asthma, bronchitis, and cardiovascular disorders) and older age can develop worst outcomes, such as chronic syndromes which require mechanical ventilation aid, or even death (1). Many studies have reported that an excessive immune reaction is responsible for patient's severe cases (Figure 4). The affectation of COVID-19 ranges from mild fatigue to multiorgan failure (13).

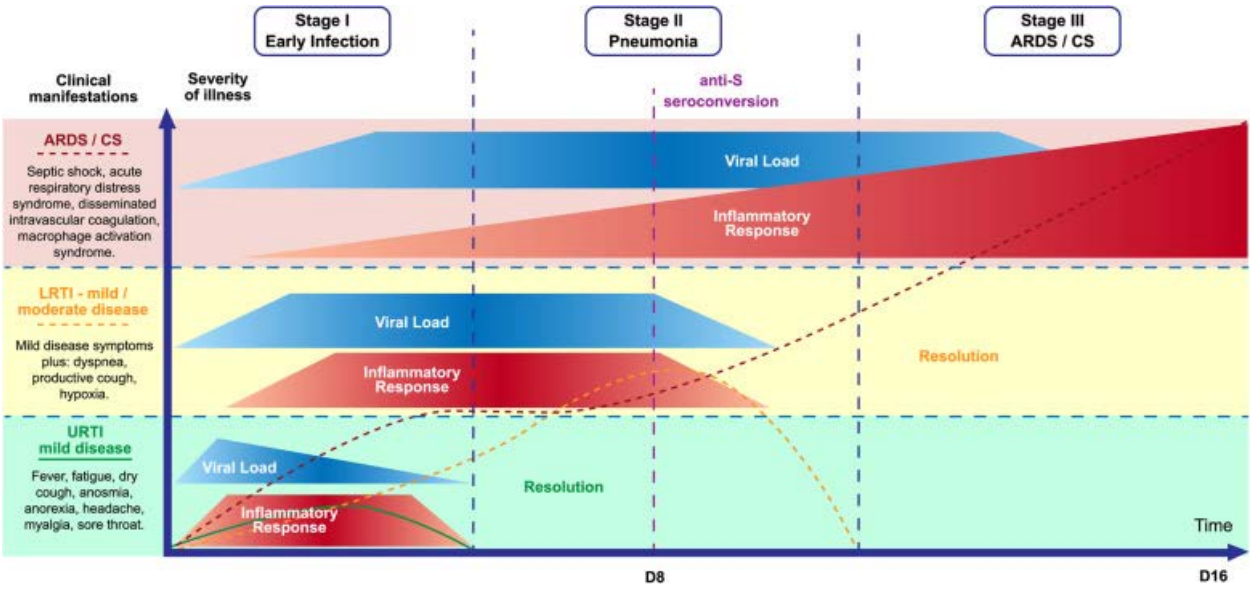

Figure 4. Spectrum of severity and stages of COVID-19. The immune system experience two stages. In the stage I, the virus inhibits the interferon production and its downstream signalling, which increase the production of inhibitory cytokines and keep the immune system suppressed. Stage II is characterized by an hyperinflammation response, which is induced by the innate immune system through a cytokine storm production. Neutrophils and monocytes/macrophages are recruited and activated in the infection site, causing collateral damage to vital organ systems. If this response is prolonged over time, stage III is triggered. Complement activation is thought to be also involved, being a link between the exaggerated innate response and the absence of an adequate immune adaptive response. All together contributes to the development of COVID-19. Extracted from Bordallo *et al*. (14).

Since the beginning of the pandemic, political authorities applied several restrictions in order to limit the virus propagation. Furthermore, the urgent for control and stop the pandemic has led to the scientific community to bring all efforts together to provide information about the virus and accelerate the development of vaccines against SARS-CoV-2. Several potential vaccines have been developed during 2020 and 2021 (Table 2)

and within less than a year they are being inoculated to population. However, after a year, the pandemic has still a major impact on global health and economy. Therefore, the worldwide vaccination is crucial for getting back to normal life as possible (15).

Table 2. Vaccine development against SARS-CoV-2. Extracted from Russell, Pelka, & Mark (16).

Type of vaccine	Vaccine's candidates
Nonreplicating viral vectors	Ad5-nCoV, ChAdOx1 nCoV-19, AD26.COV2-S, Sputnik V
Inactivated virus vaccines	PiCoVacc, BBIBP-CorV, ChiCTR2000031809
Recombinant protein subunit vaccines	NVX-CoV2373
DNA vaccines	INO-4700
RNA vaccines	mRNA-1273, BNT162b mRNA

2.1. Variants of SARS-CoV-2

Currently, another global threat is the outbreak of SARS-CoV-2 variants. As RNA viruses are characterized by high mutation rates (17), several variants of SARS-CoV-2 have already emerged in different countries. Variants with concerning epidemiological, immunological or pathogenic properties are considered as variants of concern (VOC). The WHO has declared five SARS-CoV-2 variants as VOC (18) (Table 3).

Table 3. Nomenclature of variants of concern (VOC) classified by the World Health Organization (WHO), which country were first identified, and which relevant mutations are present in spike (S) gene. Last update was on 3rd June 2021.

Pango lineage	WHO label	Country first detected	Spike mutations at interest
B.1.1.7	Alpha	United Kingdom	N501Y, D614G, P681H
B.1.1.7 + E484K	Alpha	United Kingdom	E484K, N501Y, D614G, P681H
B.1.351	Beta	South Africa	K417T, E484K, N501Y, D614G, A701V
P.1	Gamma	Brazil	K417T, E484K, N501Y, D614G, H655Y
B.1.617.2	Delta	India	L452R, T478K, D614G, P681R

SARS-CoV-2 B.1.1.7 variant was first detected in South East England on 20th September 2020. Since then, it had been spreading to over 30 countries and it became the predominant variant in March 2021 (Figure 5). The first cases reported in Spain were 19-20th December 2020 (19). This variant is characterized by a high transmission rate (20) and it has different mutations, several of which are located in S gene. The main mutations are N501Y (substitution of amino acid asparagine to tyrosine at position 501 in S gene), and 69-70del (deletion of 6 bases coding for histidine and valine at positions 69 and 70, respectively, in S gene). It is known that these two mutations had been spreading separately and independently prior to the B.1.1.7 variant emergence (21). N501Y is one of the mutations responsible for the enhanced SARS-CoV-2 transmission due to an increase affinity between viral S protein and host ACE2 receptor binding. Furthermore, it has evolved convergently, as it is also found in B.1.351 and P.1 variants (22). 69-70del mutation is also involved in increased binding affinity to the host receptor and it spontaneously evolved in other variants. This mutation is of great concern as it has the potential to enhance the ability of SARS-CoV-2 to tolerate mutations and could result in new variants with vaccine resistance properties (23). 69-70del and N501Y mutations, mainly, have allowed B.1.1.7 variant to increase the transmissibility of up to 71%. Furthermore, several cohort studies have determined an increase in mortality in patients infected with this variant compared to SARS-CoV-2 (24,25). It was reported that B.1.1.7 variant do not decrease the efficacy of current vaccines against SARS-CoV-2 (26,27).

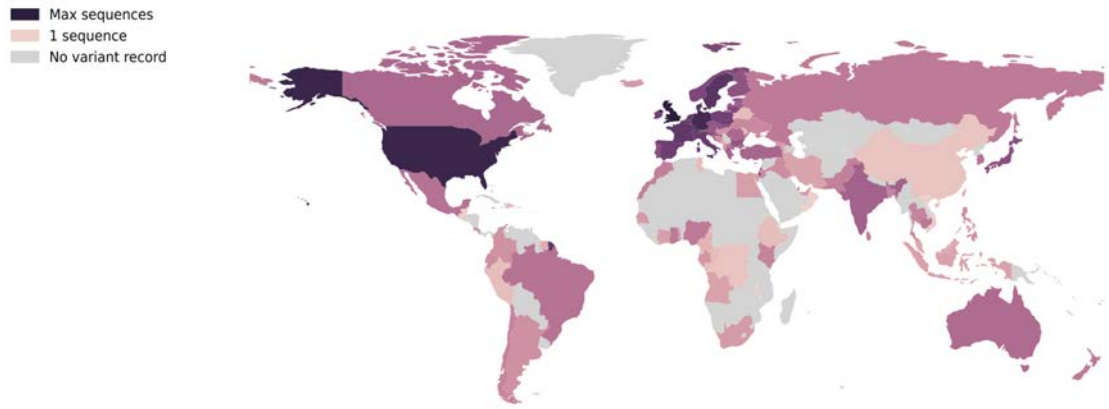

Figure 5. Logged number of sequences of SARS-CoV-2 B.1.1.7 variant in each country. Countries with more sequences logged are shown in darker colours, which implies more positive cases of the variant. Extracted from Pango lineages (28).

SARS-CoV-2 B.1.351 variant was first identified on 1st September 2020 in South Africa, where it rapidly became dominant and spread to other countries (40 countries on 11th February 2021) (Figure 6) (29,30). The first case detected in Spain was 21st January 2021 (31). Although SARS-CoV-2 B.1.351 and B.1.1.7 variants emerged independently, they share some mutations and an increased transmission capacity. B.1.351 variant present some mutations of concern in the S gene, such as K417N, E484K, and N501Y. It was also reported a deletion of three amino acids at residues 241-243, which is used for its diagnostic (32). As well as B.1.1.7 variant, N501Y allows a higher S protein binding affinity to ACE2 host receptor and it is responsible for a faster virus spread. E484K mutation is a great of concern as it interrupts interactions with most of the antibodies generated due to the vaccine (33), resulting in a significant vaccine efficacy reduction against SARS-CoV-2 (34). Furthermore, the risk of hospitalization and admission to intensive care is increased in B.1.351 variant, and it is remarkably higher in this variant as compared to B.1.1.7 and P.1 variants (35) (Table 4).

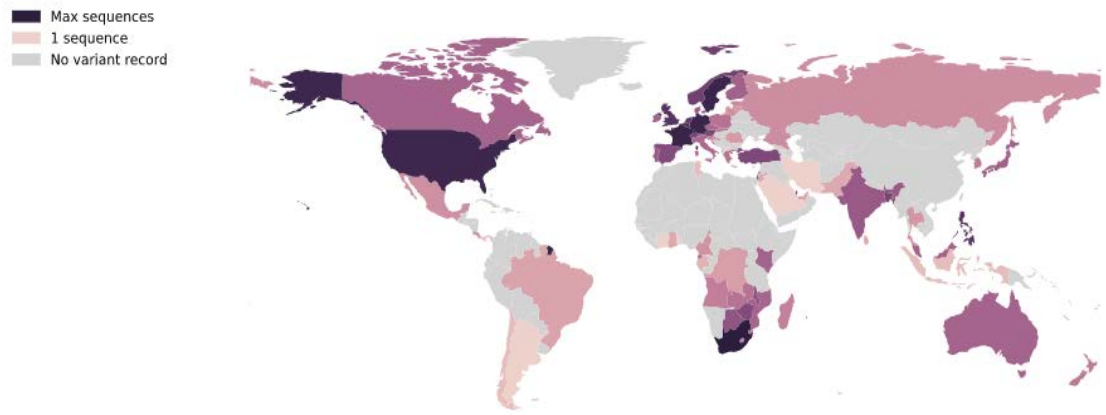

Figure 6. Logged number of sequences of B.1.351 variant in each country. Countries with more sequences logged are shown in darker colours, which implies more positive cases of the variant. Extracted from Pango lineages (30).

Table 4 . Risk of hospitalization and admission to intensive care in people infected with VOCs, such as SARS-CoV-2 B.1.1.7, B.1.351 and P.1 variants, as compared to people infected with non-VOC. Extracted from Funk *et al.* (35).

	Risk of hospitalization	**Risk of intensive care admission**
B.1.1.7 variant	1.7	2.3
B.1.351 variant	3.6	3.3
P.1 variant	2.6	2.2

Most vaccines developed are designed to generate antibody responses against the S protein of SARS-CoV-2, whereas some mutations of the new variants are located in this protein. These mutations allow new variants to escape from the host immune responses and, as a consequence, the concern about new variants outbreak is extremely increased due to the vaccine's effectiveness could be compromised. In addition, the risk of developing the severe disease is greatly increased in patients infected with VOC, as compared to non-VOC (35). Therefore, new variants emergence threatens to reverse the significant progress made so far in limiting SARS-CoV-2 transmission (36).

2.2. RT-qPCR

The need for SARS-CoV-2 detection methods has been greatly increased and the fast viral propagation of the new variants required that these methods must be reliable and quick. There are many diagnostic assays for SARS-CoV-2, such as nucleic acid amplification tests (NAAT), antigen or antibody detection, and genomic sequencing. However, the WHO determined that, wherever possible, suspected active infections should be tested with NAAT targeting SARS-CoV-2 genome, such as quantitative reverse transcription polymerase chain reaction (RT-qPCR). According to the WHO, RT-qPCR is the gold standard method to detect SARS-CoV-2 (37). Although RT-qPCR has expensive costs (38,39), it has greatly more sensitivity than antigen or antibody tests to detect the virus, whose low sensitivity makes them unsuitable methods for diagnosis (38,39). In another hand, SARS-CoV-2 genome sequencing has already demonstrated its usefulness in identifying SARS-CoV-2 as the causative agent of COVID-19 and in investigating its global spread. It has also helped to design diagnostic tools, drugs and vaccines, and to identify the outbreak of SARS-CoV-2 variants. However, its cost and work required are very high and not affordable for all laboratories. For all these reasons, RT-qPCR is the best diagnostic assay for SARS-CoV-2 pandemic.

RT-qPCR is a molecular biology technique that amplifies and detects low concentrations of ribonucleic acid (RNA) within a thermocycler. Reverse transcription and PCR reaction can take place within the same tube, called One-step RT-qPCR. Firstly, the reverse transcriptase enzyme converts RNA into cDNA. Then, the three basic steps of a PCR take place, such as DNA denaturation, annealing and extension. Each step is characterized by different temperature and time to allow double-stranded DNA separation, primers hybridization with its complementary target and nucleotides addition by DNA polymerase, respectively. The current fashion is to perform annealing and elongation in the same step, this is possible when the primer melting temperature (T_m) is close to the extension temperature (40). The three steps are repeated consecutively many times (40-45 cycles) and the amount of DNA doubles with each cycle. RT-PCR allows SARS-CoV-2 detection, but as samples viral load also needs to be quantified, a RT-qPCR methodology is performed. The quantification can be based on different technologies, such as TaqMan probes (Figure 7).

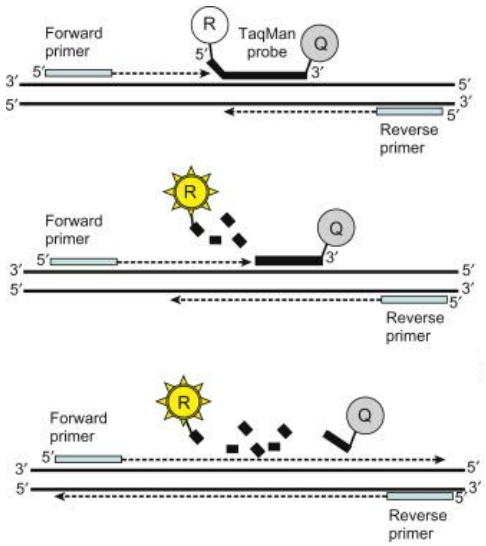

Figure 7. TaqMan technology. The TaqMan probe incorporates a 5′ reporter, which is a fluorescent dye, and a 3′ non fluorescent quencher, which absorbs the fluorescence emission of the reporter. During the PCR annealing/extension step, the probe hybridizes with the target region and the reporter's fluorescence is suppressed by the quencher. When DNA polymerase elongates the primer, its 5′-3′ exonuclease activity cause probe degradation and the reporter is released, allowing fluorescence emission that will be measured by the thermocycler during the RT-qPCR assay.

The RT-qPCR results are provided as threshold cycle (C_t) values and amplification plots, which results from plotting relative fluorescence (ΔRn) against PCR number cycles (Figure 8). The thermocycler set in each reaction a threshold line where the fluorescence signal is maintained equally, and it is caused by the background (baseline fluorescence). The C_t value corresponds to the cycle number where is recorded the first fluorescent signal which is statistically significant and above the baseline. Graphically, it is the point at which the amplification plot crosses the threshold line. As more nucleic acid present in the sample, fewer cycles will be necessary to reach the C_t. C_t values are used to interpret the results as positive or negative in SARS-CoV-2 infection (47). RT-qPCR has routinely been used to confirm positive cases of SARS-CoV-2 infection throughout the pandemic (48).

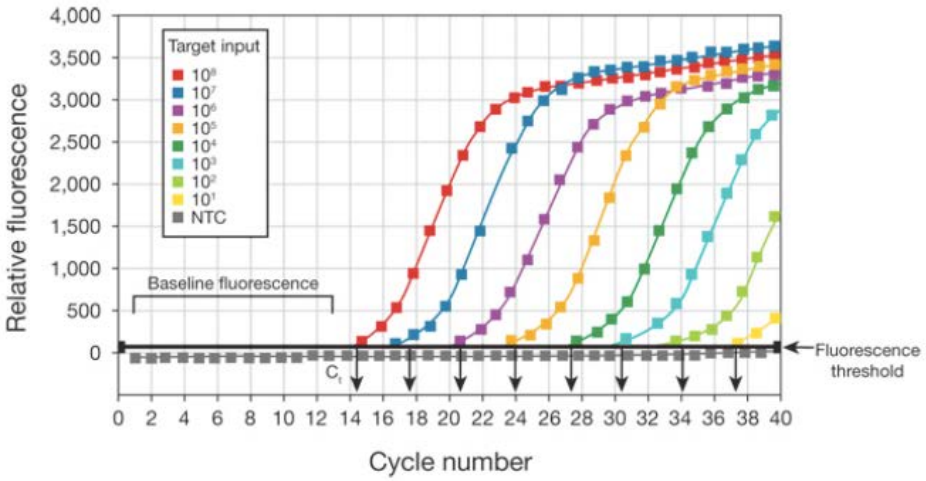

Figure 8. Amplification plot generated from plotting relative fluorescence against cycles number. Each curve corresponds to a different target. Relative fluorescence is calculated automatically by the instrument according to the following formula: $\Delta Rn = Rn^+ - Rn^-$ (Rn^+ = reporter emission intensity/ quencher emission intensity at any given time in the reaction tube. Rn^- = reporter emission intensity/ quencher emission intensity measured prior to PCR amplification in the same reaction tube). Extracted from Life technologies (41).

2.3. RT-qPCR in wastewater samples

Since the beginning of SARS-CoV-2 pandemic, routinary analysis of wastewater samples have been performed to detect the viral load in different geographical areas (42,43). This is possible due to SARS-CoV-2 remains in human faeces though several days, more than in respiratory samples. It was reported that faeces from people who had been infected with SARS-CoV-2 remain positive up to 33 days after a negative nasopharyngeal swab (44). Firstly, it was considered SARS-CoV-2 transmission through faecal-oral route. However, the risk of transmission via wastewater and surficial waters, such as rivers, was demonstrated to be insignificant due to the virus lacks its infection capacity (45,46). The virus loses infectivity in the human gastrointestinal tract due to the colonic fluid (47). Therefore, wastewater samples can be used to monitor the viral spreading without any health risk. Wastewater samples, collected from wastewater treatment plants (WWTP) or city sewers, serve as an early warning of infection hotspots due to it is capable to detect SARS-CoV-2 weeks before the first confirmed case by nasopharyngeal samples. Furthermore, patients without any clinical symptoms remain undiagnosed, but as viral RNA remains in their faeces, they can be identified by wastewater analysis. Therefore, this early detection of the virus through wastewater analysis could be used to limit the viral spreading and it is a successful strategy to monitor the infection propagation in specific population (48).

3. HYPOTHESIS AND OBJECTIVES

Since the beginning of the pandemic, SARS-CoV-2 has been routinely identified through RT-qPCR in patients with clinical symptoms. However, a large percentage of asymptomatic patients remain undiagnosed. Wastewater analysis through RT-qPCR allows closer monitoring of infected patients due to SARS-CoV-2 remain in their faeces for several days. Therefore, analysis of wastewater samples collected from city sewers or wastewater treatment plants allows monitoring positive and asymptomatic cases of SARS-CoV-2, as well as its variants.

The aim of this project is to detect SARS-CoV-2 B.1.1.7 and B.1.351 variants in wastewater samples through RT-qPCR methodology. For this, methods based on Vogels *et al.* (49) methodology to detect 69-70del mutation of SARS-CoV-2 B.1.1.7 variant, and Yaniv *et al*. (50) methodology to detect 241-243del mutation of SARS-CoV-2 B.1.351 variant were optimized. Standardisation of the detection methods was also conducted to allow quantification of the variants genomic load per litre of wastewater.

4. METHODS

RT-qPCR assays were performed to detect SARS-CoV-2 B.1.1.7 and B.1.351 variants in wastewater samples. Firstly, the samples were collected by staff members on city sewers and sewage treatment plants and transported to the laboratory in refrigeration (4°C) to avoid RNA degradation, according to ISO 5667-3:2012. Once in the laboratory, samples were submitted to different methodologies before RT-qPCR takes place, such as concentration and RNA extraction. An internal control was needed to ensure that the whole process is carried out correctly. This control consists of Mengovirus addition to samples at the beginning of the concentration process in order to know which percentage of Mengovirus was recovered after the whole methodology. It had been established to obtain a Mengovirus recovery percentage higher than 1 to guarantee a successful RNA extraction, following ISO 15216-1:2017(E) indications. The election of the virus control was also carried out also according to ISO 15216-1:2017(E). Finally, the extracted RNA was submitted to RT-qPCR to detect and quantify SARS-CoV-2 variants.

4.1. Concentration

Wastewater samples are composed of suspended solids and organic matter residues, mainly. This results in highly complex matrices and, as a consequence, a low concentration of SARS-CoV-2 and its variants is present. Therefore, a concentration process is required. This protocol was created in collaboration with the CSIC-IATA and based on Randazzo *et al.* protocol (48).

Samples were received in the laboratory and poured into bottles of 200 mL (Figure 9). The process started by adding 100 µL of a Mengovirus solution (1/1000 diluted) to 200 mL bottles. The pH was adjusted to 6 and 2 mL of 0.9 N $AlCl_3$ solution were added to each sample. The pH was adjusted again to 6. Bottles were submitted to agitation at 150 rpm for 15 minutes, followed by 2700 rpm centrifugation for 20 minutes. Then, the supernatant was discarded, and the pellet was resuspended in 10 mL of 3% meat extract. Samples passed from 200 mL bottles to 15 mL falcon tubes. Falcon tubes were agitated at 200 rpm for 10 minutes and centrifugated at 2900 rpm for 30 minutes. Finally, the supernatant was again discarded, and the pellet was resuspended in 1 mL of Phosphate Buffered Saline (PBS), leading to concentrated samples. The final volume of concentrated samples was 2 mL, approximately.

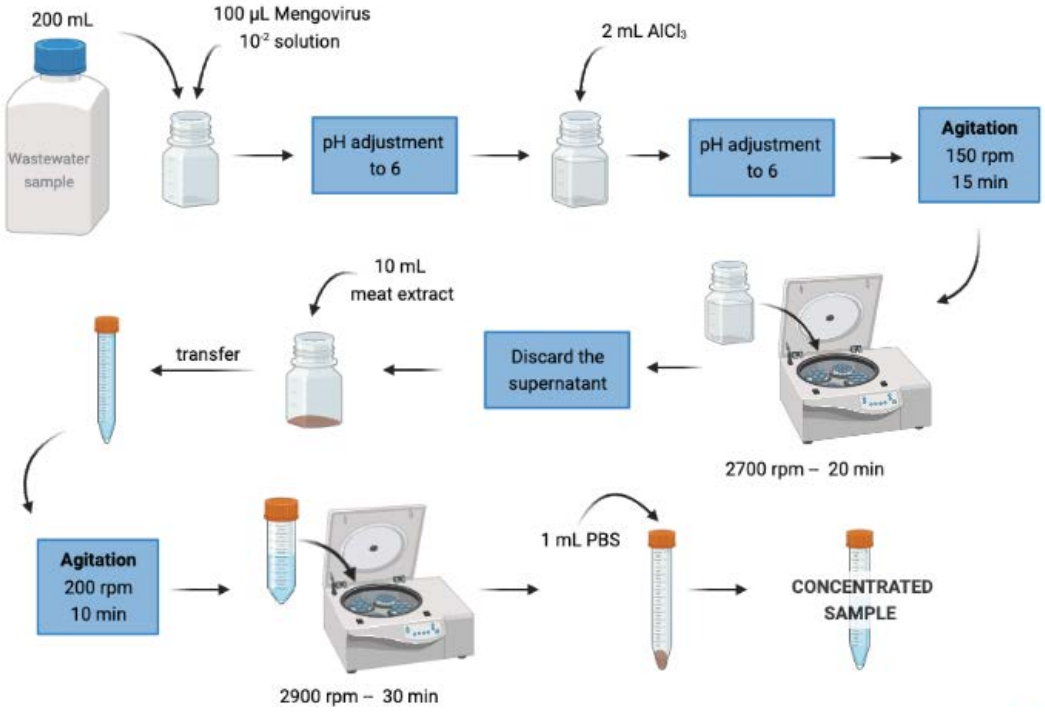

Figure 9. Diagram of the wastewater samples concentration process. Created with Biorender.

4.2. Extraction

The RNA extraction process (Figure 10) was performed with NucleoSpin™ RNA Virus Kit (Macherey-Nagel), according to the manufacturer's protocol. The process was started by adding 600 μL of RAV1, 25 μL of Plant RNA Isolation Aid and 150 μL of each sample to Eppendorf tubes. It was important to clean the pipette between samples deposition to avoid cross-contamination. Then, the tubes were vortexed and centrifugated at 10000 rpm for 5 minutes. The supernatant was deposited in a new Eppendorf tube and incubated at 70°C for 5 minutes. After incubation, 600 μL of ethanol were added to each sample. It was important to perform this step as fast as possible to stop cellular lysis. 700 μL of Eppendorf tubes content were deposited into an extraction column and centrifugated at 8000 rpm for 1 minute. The eluate was discarded and the rest of the tube content was deposited in the same column. It was centrifugated at 8000 rpm for 1 minute and the eluate was discarded again. At this point, the RNA was bound to the column and, from here, a wash process was started. 500 μL of RAW were added to the column and it was centrifugated at 8000 rpm for 1 minute, followed by eluate discarding. This process was repeated firstly with 600 μL of RAV3 and secondly with 200 μL of RAV3. After these wash steps, the column was deposited into an Eppendorf tube and 50 μL of RNase-free water pre-heated at 70°C were added to the column. Tubes were left at room temperature for 1 minute. Finally, Eppendorf tubes with respective columns were centrifugated at 11000 rpm for 1 minute. Columns were discarded and RNA was obtained in the eluate (50 μL).

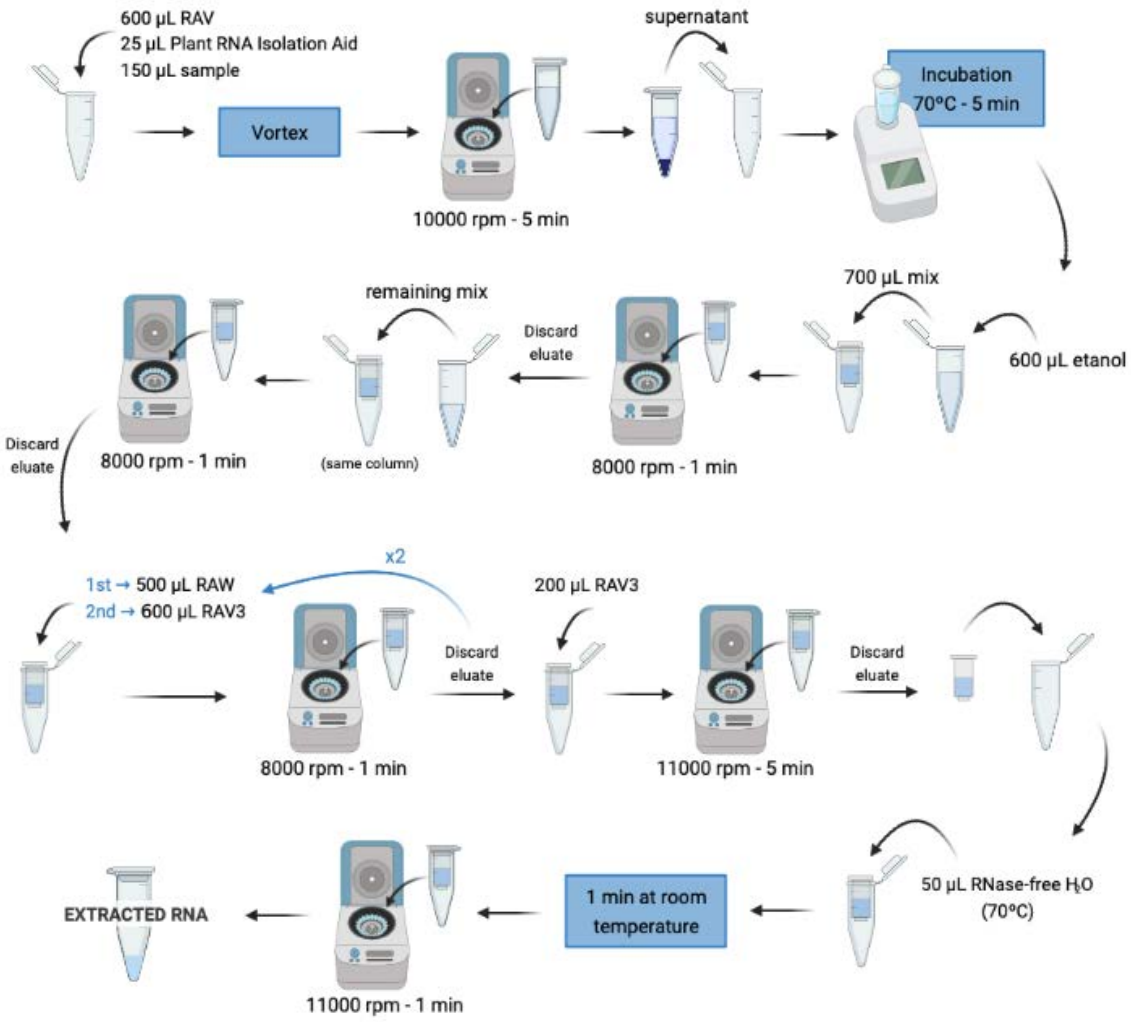

Figure 10. Diagram of RNA extraction with NucleoSpin™ RNA Virus Kit (Macherey-Nagel). Created with Biorender.

4.3. RT-qPCR

4.3.1. SARS-CoV-2 B.1.1.7 variant

The RT-qPCR was performed with One Step PrimeScript™ RT-PCR Kit (TaKaraBio Inc.) using QuantStudio™ 5 Real-Time PCR System (ThermoFisher). The master mix was prepared according to the manufacturer's protocol, and primers and probes concentration were specified by Vogels *et al.* protocol (49) (multiplex reaction in Table 5, single reaction in Table 6). According to the final required concentration of primers, probes and RNA, the RNase-free water volume was adapted. A positive control of B.1.1.7 variant and SARS-CoV-2 original was used (reference material), as well as a negative control (RNase-free water). Controls were added to each RT-qPCR performed.

Thermal cycling conditions were carried out using a transcriptase reverse step of 55°C for 10 min, followed by reverse transcriptase deactivation of 95°C for 1 min. Then, 45 cycles of denaturation at 95°C for 10 sec, and annealing and extension at 60°C for 45 sec (optimized conditions).

Table 5. Volume of each reagent added to the RT-qPCR master mix in a final volume of 20µL. A multiplex reaction was performed with 69-70del and Wuhan probes. The final concentration of primers and probes were specified by Vogels *et al*. protocol (49).

Reagent	Volume (µL)	Final concentration (µM)
2X One Step RT-PCR Buffer III	10	1X
TaKaRa Ex Taq HS	0.4	
PrimeScript RT enzyme Mix II	0.4	
ROX Reference Dye II	0.4	
RNase Free dH2O	1.88	
Forward Primer (10 µM)	0.8	0.4
Reverse Primer (10 µM)	0.8	0.4
69-70del Probe (25 µM)	0.16	0.2
Wuhan Probe (25 µM)	0.16	0.2
RNA	5	
TOTAL	20	

Table 6. Volume of each reagent added to the RT-qPCR master mix in a final volume of 20µL. A single reaction was performed with 69-70del probe. The final concentration of primers and probes were specified by Vogels *et al*. protocol (49).

Reagent	Volume (µL)	Final concentration (µM)
2X One Step RT-PCR Buffer III	10	1X
TaKaRa Ex Taq HS	0.4	
PrimeScript RT enzyme Mix II	0.4	
ROX Reference Dye II	0.4	
Rnase Free dH2O	2.04	
Forward Primer (10 µM)	0.8	0.4
Reverse Primer (10 µM)	0.8	0.4
69-70del Probe (25 µM)	0.16	0.2
RNA	5	
TOTAL	20	

Primers and probe to detect B.1.1.7 variant were design to hybridize with 69-70 deletion (69-70del), a characteristic mutation of this variant. Information about primers and probes is shown in Table 7 and Table 8.

Table 7. Information about primers and probes used in the RT-qPCR assay to detect B.1.1.7 SARS-CoV-2 variant.

	Nt positions	TM (°C)	Length (nt)	Sequence (5' to 3')
Forward primer	21,710-21,733	59,3	24	TCAACTCAGGACTTGTTCTTACCT
Reverse primer	21,796-21,817	57,4	22	TGGTAGGACAGGGTTATCAAAC
Wuhan probe	21,755-21,779	61,2	25	TTCCATGCTATACATGTCTCTGGGA
69-70del probe	21,752-21,782	65,1	25	TGGTTCCATGCTATCTCTGGGACCA

Table 8. Information about probes used in RT-qPCR assay to detect B.1.1.7 SARS-CoV-2 variant.

Probe	Gene	Reporter	Quencher
Wuhan	S gene (wild-type)	FAM	BHQ2
69-70del	S gene (69-70del)	HEX	BHQ2

PCR reagents and thermocycler used differ from Vogels *et al*. protocol (49). Therefore, PCR programme conditions according to this protocol were not specific for the own laboratory equipment. Different probes were taken to adequate the PCR programme to instrument and PCR kit used in the own laboratory. Furthermore, a calibration method was developed to quantify the samples content of SARS-CoV-2 and variants in genomic units per litre (GU/L). Once the detection method was optimized and standardised, real samples were analysed.

4.3.2. SARS-CoV-2 B.1.351 variant

RT-qPCR was performed in same conditions as SARS-CoV-2 B.1.1.7 variant, with One Step PrimeScript™ RT-PCR Kit (TaKaraBio Inc.) using QuantStudio™ 5 Real-Time PCR System (ThermoFisher). The master mix was prepared according to the manufacturer's protocol, and primers and probe concentration were specified by Yaniv *et al*. protocol (Table 9) (50). According to the final required concentration of primers, probes and RNA, the RNase-free water volume was adapted. A positive control of B.1.351 variant

(reference material) and a negative control (RNase-free water) were used. Controls were added to each RT-qPCR performed. Thermal cycling conditions were carried out using a transcriptase reverse step of 50°C for 10 min, followed by reverse transcriptase deactivation of 95°C for 3 min. Then, 45 cycles of denaturation at 95°C for 3 sec, and annealing and extension at 55°C for 45 sec (optimized conditions). The primers and probe to detect B.1.351 variant were designed to hybridize with 241-243 deletion (241-243del). Information about primers and probes is shown in Tables 10 and 11.

Table 9. Volume of each reagent added to the RT-qPCR master mix in a final volume of 20µL. The final concentration of primers and probe were specified by Yaniv *et al*. protocol (50).

Reagent	Volume (µL)	Final concentration (µM)
2X One Step RT-PCR Buffer III	10	1X
TaKaRa Ex Taq HS	0.4	
PrimeScript RT enzyme Mix II	0.4	
ROX Reference Dye II	0.4	
RNase Free dH2O	1.4	
Forward Primer (10 µM)	1	0.5
Reverse Primer (10 µM)	1	0.5
241-243del Probe (25 µM)	0.4	0.2
RNA	5	
TOTAL	20	

Table 10. Information about primers and probes used in RT-qPCR assay to detect B.1.351 SARS-CoV-2 variant.

	Sequence (5' to 3')
Forward primer	AGATTTGCCAATAGGTATTAACATC
Reverse primer	CTGAAGAAGAATCACCAGGAGTC
Probe 241-243 del	FAM-CTAGGTTTC/ZEN/AAACTTTACATAGAAGTT-BHQ2

Table 11. Information about probe used in RT-qPCR assay to detect B.1.351 SARS-CoV-2 variant.

Probe	Gene	Reporter	Quencher
241-243del	S gene (241-243del)	HEX	BHQ2

In the same way as SARS-CoV-2 B.1.1.7 variant, optimization of the RT-qPCR to detect SARS-CoV-2 B.1.351 variant was performed due to reagents and instrument differ from Yaniv *et al.* protocol (2).

5. RESULTS

5.1. Optimization of the methods

The methods to detect SARS-CoV-2 variants, such as B.1.1.7 and B.1.351 lineages, required a prior optimization due to results with conditions stablished by the respective authors (49,50) reveals a lack of specificity in the RT-qPCR reaction. For this reason, different tests were performed to improve the reactions specificity. The results obtained in the respective RT-qPCR were analysed with the Design and Analysis Software provided by the thermocycler manufacturer (ThermoFisher). This software allows modification of RT-qPCR conditions prior to its performance and provides C_t value and amplification plot for each sample.

5.1.1. SARS-CoV-2 B.1.1.7 variant

The optimization of SARS-CoV-2 B.1.1.7 variant detection method started with RT-qPCR conditions specified by Vogels *et al.* protocol (49) (Table 12). The 69-70del probe was expected to detect B.1.1.7 variant as it was designed to hybridize with 69-70del mutation present in S gene. In another hand, the Wuhan probe was expected to detect original SARS-CoV-2, as it was designed to hybridize with the wild-type sequence. In each tests, control for B.1.1.7 variant and original SARS-CoV-2 (Wuhan) were used.

Table 12. RT-qPCR conditions, such as repetitions, temperature, and time specified by Vogels *et al.* protocol (49) in each RT-qPCR step to detect B.1.1.7 variant of SARS-CoV-2.

	Cycles	Temperature	Time
Reverse transcription	1	55°C	10 min
Reverse transcriptase inactivation	1	95°C	1 min
PCR (denaturation, annealing-extension)	45	95°C	10 s
		55°C	30 s

After performing RT-qPCR with conditions present in Table 12, the results showed an unspecific amplification and evidenced poor sensitivity (Figures 11 and 12). These figures showed non-specific curves corresponding to the positive control that was not being amplified. Different tests were performed to improve the reaction sensitivity and obtain amplification plots with only the corresponding curve.

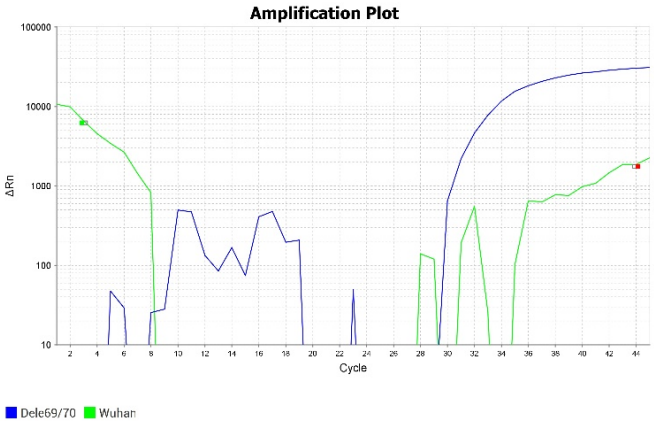

Figure 11. Amplification plot of positive SARS-CoV-2 B.1.1.7 variant control (blue curve). It is possible to visualize an unspecific curve corresponding to original SARS-CoV-2 (green curve). RT-qPCR performed with initial conditions.

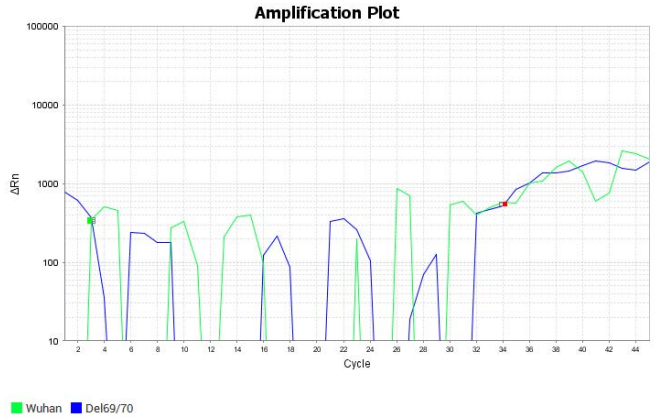

Figure 12. Amplification plot of positive original SARS-CoV-2 control (green curve). It is possible to visualize a curve corresponding to SARS-CoV-2 B.1.1.7 variant (blue curve). RT-qPCR performed with initial conditions.

Firstly, the time of reverse transcription step was changed from 10 to 20 minutes. Results evidenced that unspecificity remains (results not shown), indicating that the reverse transcription step was not a critical point, and the time of these step was maintained at 20 min. To achieve better results, annealing step conditions are usually modified. As annealing and extension were designed to be in the same step, the

temperature of this step was increased from 55°C to 60°C. The RT-qPCR reaction specificity was improved, as better results were obtained with 60°C than 55°C (Figures 13 and 14). However, further optimizations were still required to achieve amplification curves more defined.

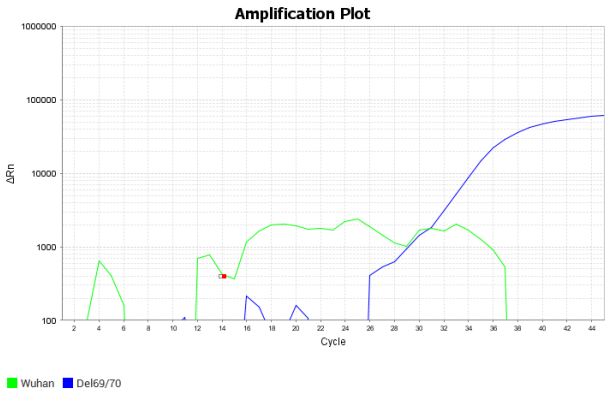

Figure 13. Amplification plot of positive SARS-CoV-2 B.1.1.7 variant control. RT-qPCR performed with increased hybridization and elongation temperature from 55 to 60°C.

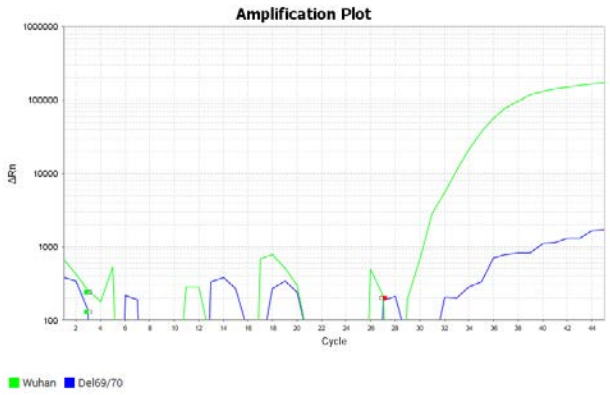

Figure 14. Amplification plot of positive Wuhan control. RT-qPCR performed with increased hybridization and elongation temperature from 55 to 60°C.

As further improvements were required, the annealing and extension temperature was again modified to 57°C and 63°C. It was observed that Wuhan control curve was not appropriate, and it did not appear signal in most of the tests carried out. For this reason, the two probes (69-70del and Wuhan) were placed separately and together to test if there was any inhibition in the multiplex reaction. No significant differences were achieved when temperature was changed to 57°C and 63°C, and better results were obtained with multiplex reaction (amplification plots not shown).

Other RT-qPCR conditions were modified, such as denaturalization time from 1 to 2 minutes, and annealing and extension time from 30 to 45 seconds. Better amplification curves were obtained with annealing and extension time increase (Figures 15 and 16). Then, annealing and extension time was tested with 1 minute, but no significantly different results were obtained in comparison to results with 45 seconds. Therefore, this step time was maintained at 1 minute.

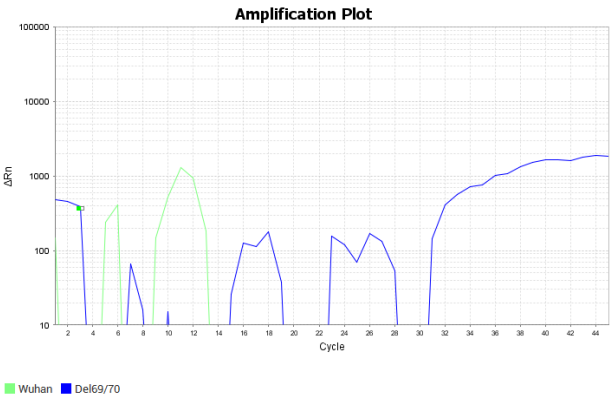

Figure 15. Amplification plot of positive SARS-CoV-2 B.1.1.7 variant control. RT-qPCR performed with increased annealing and extension time from 30 to 45s.

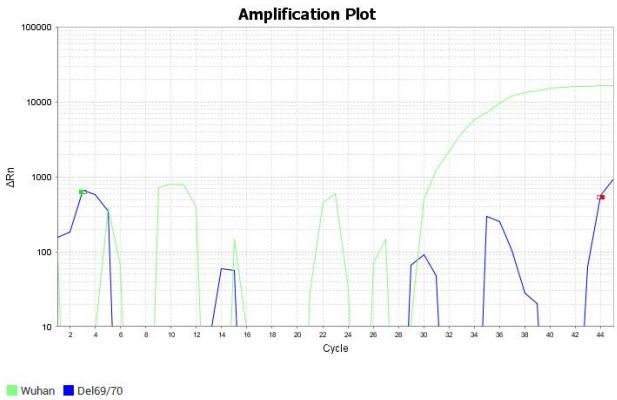

Figure 16. Amplification plot of positive Wuhan control. RT-qPCR performed with increased annealing and extension time from 30 to 45s.

After all RT-qPCR conditions were modified, amplification plots still required further improvement. It was decided to modify conditions of RT-qPCR master mix reagents. The unique reagent with possibility to be modified was ROX. ROX standardises the fluorescent reporter signal and it was used diluted 1/100. Firstly, it was tested with dilutions 1/50 and 1/10. After no improvement obtained, ROX was tested diluted 1/5, 1/2 and undiluted, showing better results when ROX was used without any dilution (Figures 17 and 18).

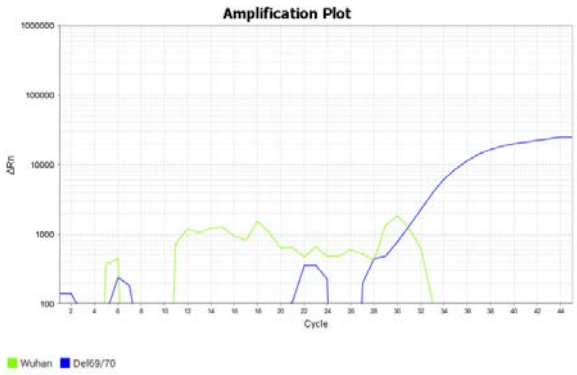

Figure 17. Amplification plot of positive SARS-CoV-2 B.1.1.7 variant control. RT-qPCR performed with ROX undiluted.

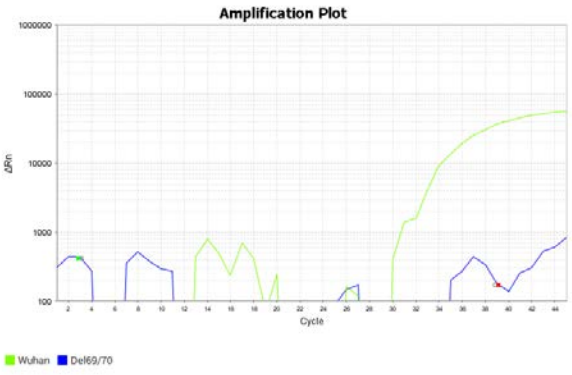

Figure 18. Amplification plot of positive Wuhan control. RT-qPCR performed with ROX undiluted.

After all the tests performed, programme conditions of RT-qPCR were established as shown in Figure 19. Changes maintained were temperature and time increase in the annealing and extension step from 55°C to 60°C and 30s to 45s, respectively, and ROX was used without dilution, instead of ten-fold diluted.

Figure 19. Schema of repeats, temperature and time conditions for each step of the RT-qPCR reaction. It is also illustrated when the instrument collects fluorescence information (final step).

5.1.2. SARS-CoV-2 B.1.351 variant

The first RT-qPCR assay for SARS-CoV-2 B.1.351 variant detection was performed with conditions specified by Yaniv *et al.* (50) protocol (Table 13) with positive control of SARS-CoV-2 B.1.351 variant (reference material) directly and ten-fold diluted, and a negative control (RNase-free water). As master mix used was the same as in B.1.1.7 variant assay, ROX was tested directly undiluted (it allowed significant improvements in SARS-CoV-2 B.1.1.7 variant method optimization).

Table 13. RT-qPCR conditions, such as repetitions, temperature, and time specified by Yaniv et al. protocol (50) in each RT-qPCR step.

	Cycles	Temperature	Time
Reverse transcription	1	50°C	10 min
Reverse transcriptase inactivation	1	95°C	3 min
PCR (denaturation, annealing-extension)	45	95°C	3 s
		55°C	30 s

The first results obtained (Figure 20) were better than first results of B.1.1.7 variant. The C_t values were 18,3 and 18,29 for direct replicates, and 20,54 and 26,38 for ten-fold diluted replicates. Although these values were adequate (as the reference material concentration was 1,000,000 GU/μL), the amplification curves required some specificity improvements. It was evidenced some shaky appearance in the plateau phase of the curves.

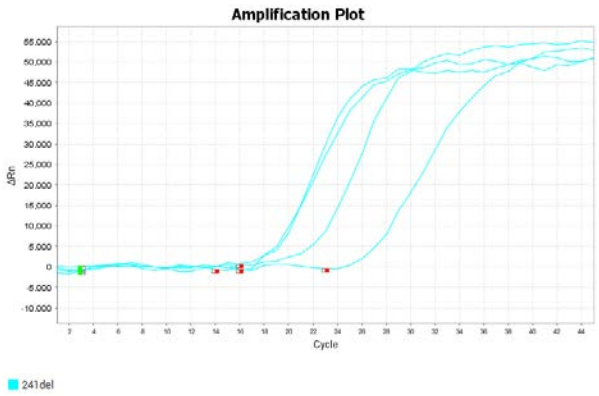

Figure 20. Amplification plot of positive SARS-CoV-2 B.1.351 variant control. Each curve represents one replicate. RT-qPCR reaction was performed with initial conditions.

To check if any reaction improvement was achieved, annealing and extension time was increased from 30 to 45 seconds. Results did not evidence shakiness (Figure 21) and C_t values were also adequate (18,65 and 19,05 for direct replicates, and 22,39 and 22,33 for ten-folded replicates). Therefore, it was decided to maintain these conditions for the detection of SARS-CoV-2 B.1.351 variant (Figure 22).

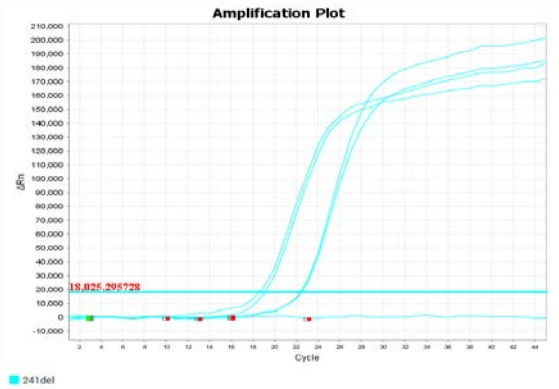

Figure 21. Amplification plot of positive SARS-CoV-2 B.1.351 variant control. RT-qPCR performed with increased annealing and extension time from 30 to 45 seconds. Two replicates of positive control direct and ten-fold diluted were tested.

Figure 22. Schema of repeats, temperature and time conditions for each step of the RT-qPCR reaction for SARS-CoV-2 B.1.351 variant detection. It is also illustrated when the instrument collects fluorescence information (final step).

5.2. Calibration of the methods

The RT-qPCR provides an amplification plot and C_t value for each sample. These data are useful to detect SARS-CoV-2 presence in samples. However, if absolute quantification of each sample is wanted, a calibration method needs to be performed. The calibration allows standardisation of samples and reference to the standard curve enables quantification of the RNA in virus genome copies per litre of wastewater sample. Therefore, the viral load of each sample will be known and not only detected.

Standardisation was performed with a reference material of SARS-CoV-2 B.1.1.7 and B.1.351 variants (the same as tests performed for methods optimization), being RNA plasmids of known concentration. Different dilution series of these plasmids were conducted, chosen in a concentration range within the detection limit of the instrument and taking into account the approximate viral concentration of samples that will be analysed. The concentrations were as follows: 250000, 25000, 2500, 250, 100, 50, 25 in genome units (GU) per µL. Five replicates of each concentration were measured by RT-qPCR with the optimized conditions described above. C_t values and

amplification plots were obtained for SARS-CoV-2 B.1.1.7 variant (Figures 23 and 24) and for SARS-CoV-2 B.1.351 variant (Figures 25 and 26).

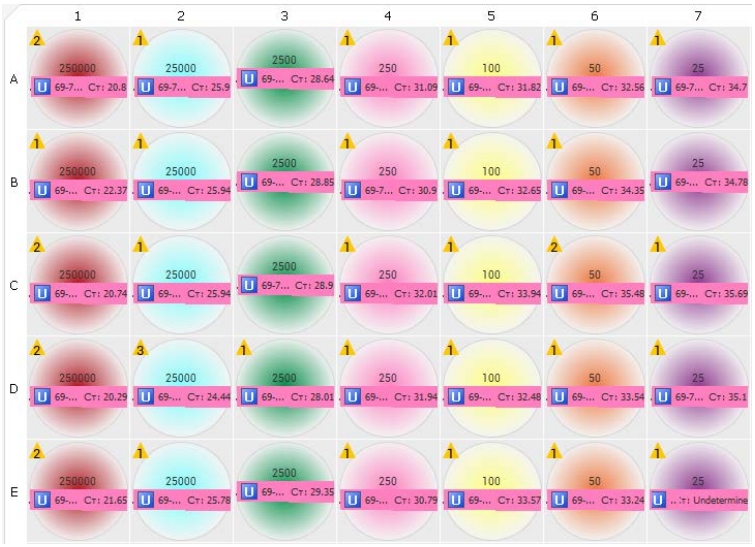

Figure 23. Calibration method of SARS-CoV-2 B.1.1.7 variant through RT-qPCR. Screenshot of instrument Design and Analysis Software where is possible to visualize replicates of each concentration with the respective C_t value. Each well corresponds to a replica of each concentration. Samples were loaded in the following order: 250000 GU/µL, 25000 GU/µL, 2500 GU/µL, 250 GU/µL, 100 GU/µL, 50 GU/µL, 25 GU/µL, and negative control (C-).

*Concentrations of 100 GU/µL and 50 GU/µL were analysed just in case 25 GU/µL could not been detected by the instrument for being almost in the instrument limit detection. However, as it was detected, these concentrations (100/µL and 50/µL) were not used to generate the calibration straight-line.

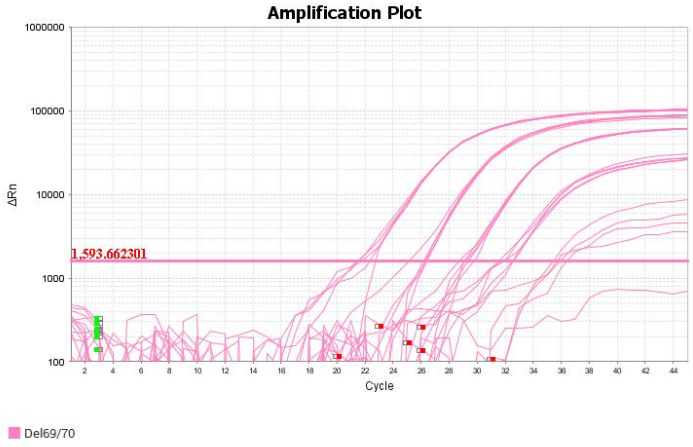

Figure 24. Amplification plot of dilution series of SARS-CoV-2 B.1.1.7 variant reference material used for calibration of SARS-CoV-2 B.1.1.7 variant method detection. The red value corresponds to the threshold value obtained in this reaction. Each curve corresponds to a replica of each concentration, in the following order 250000, 25000, 2500, 250 and 25 GU/µL from left to right, respectively.

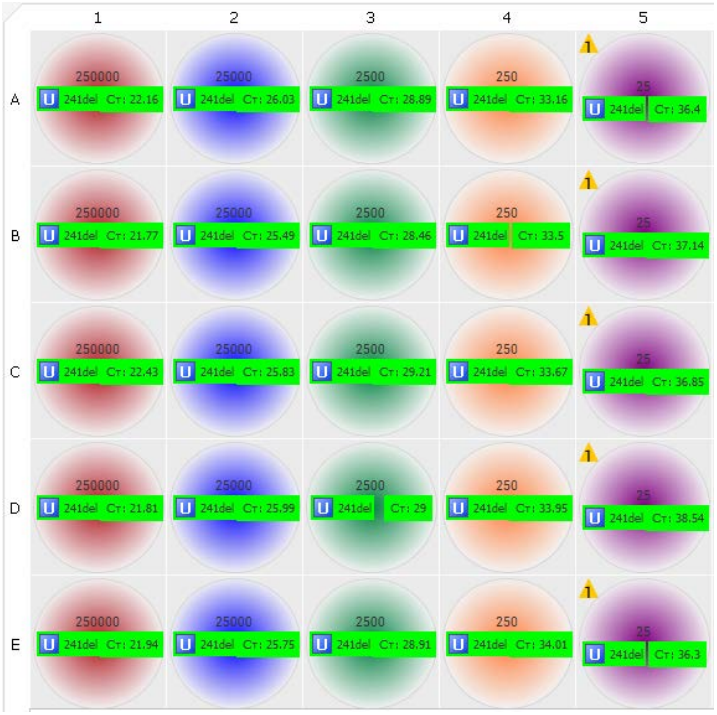

Figure 25. Calibration method of SARS-CoV-2 B.1351 variant through RT-qPCR. Screenshot of instrument *Design and Analysis Software* where is possible to visualize replicates of each control concentration with the respective C_t value. Each well corresponds to a replica of each concentration. Samples were loaded in the following order: 250000 GU/µL, 25000 GU/µL, 2500 GU/µL, 250 GU/µL, 25 GU/µL, and negative control (C-).

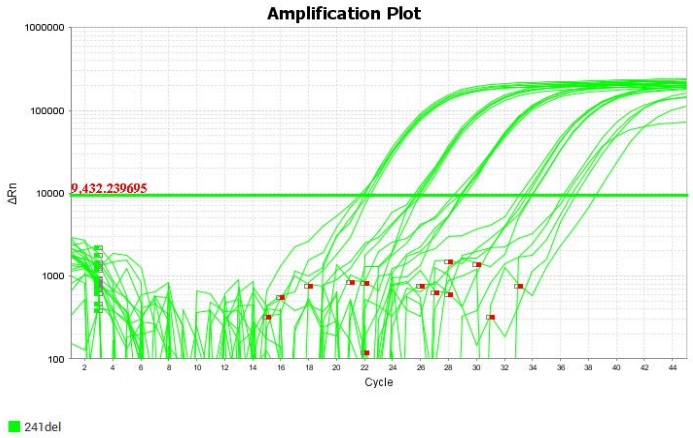

Figure 26. Amplification plot of dilution series of SARS-CoV-2 B.1.351 variant reference material used for calibration of SARS-CoV-2 B.1.351 variant method detection. The red value corresponds to the threshold value obtained in this reaction. Each curve corresponds to a replica of each concentration, in the following order 250000, 25000, 2500, 250 and 25 GU/µL from left to right, respectively.

Furthermore, as different employees will perform the RT-qPCR methodology to analyse wastewater samples content of SARS-CoV-2 variants, different calibrations were conducted (four in total), so that differences in work between individuals do not

affect quantification (in the previous figures only one result of four measures are shown). Four calibration measures were performed for each SARS-CoV-2 variant, and twenty replicates of each concentration were measured in total (5 replicates per trial). Average of C_t values obtained in each trial were calculated and also the standard deviation. Then, the C_t value average for each concentration were plotted against $\log_{10}$ of the target concentrations, and a calibration straight-line was generated with a negative slope for each SARS-CoV-2 variant (Figures 27 and 28), following the ISO 15216-1:2017(E) indications. Person's correlation coefficient (r^2), slope and intercept parameters were calculated. The slope and intercept parameters allow quantification of viral genome units per litre of wastewater sample, and it was used to quantify SARS-CoV-2 B.1.1.7 and B.1.351 variants load in each sample.

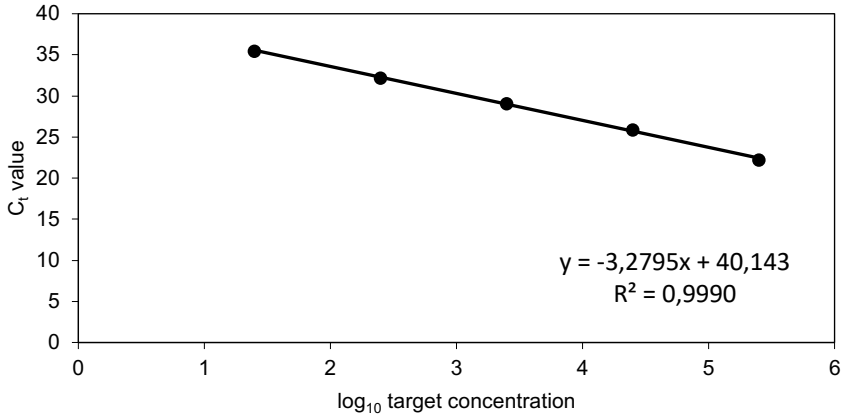

Figure 27. Calibration straight-line and slope, intercept and r^2 value obtained in the method standardisation of SARS-CoV-2 B.1.1.7 variant.

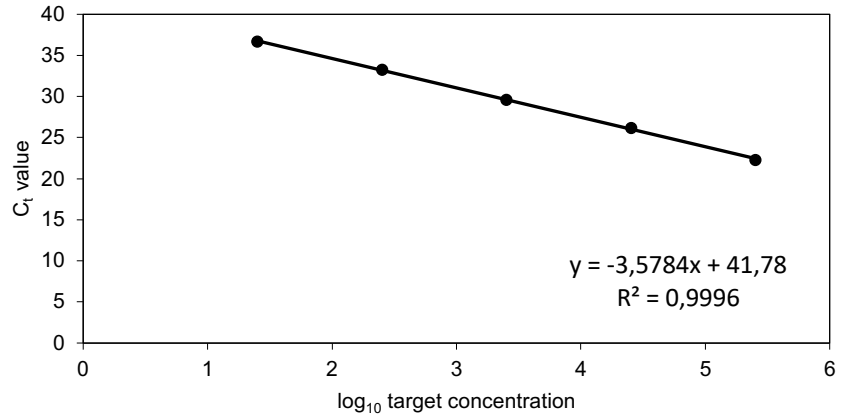

Figure 28. Calibration straight-line and slope, intercept and r^2 value obtained in the method standardisation of SARS-CoV-2 B.1.351 variant.

5.3. Results interpretation

Samples results have to be interpreted as positive, negative or inconclusive according to the C_t value and amplification plot provided by the thermocycler software. Firstly, the C_t values were analysed according to Table 14.

Table 14. Interpretations of results according to the C_t value obtained in the RT-qPCR, following the instrument manufacturer's manual.

C_t value	Result interpretation
$C_t < 38$	Positive
$38 \leq C_t < 40$	Inconclusive
C_t = undetermined	Negative

Secondly, the amplification graph was analysed to corroborate the results interpretation, where an exponential curve with a plateau phase should be observed. If the outcome was unclear, the amplification curve was analysed in comparison with the positive control curve of each SARS-CoV-2 variant. If sample and control curves were similar, the result was interpreted as positive (Figures 29, 30 and 31 show positive result for B.1.1.7 variant, original SARS-CoV-2 and both, respectively), whereas if non-similarities were observed, the result was interpreted as negative (an example is shown in Figure 32). Checking amplification plots is important to detect false-positives results, identified with very low C_t values (for example 10) or amplification curves with no exponential phase. Examples of false-positive results are shown in Figures 33.1, 33.2 and 34.

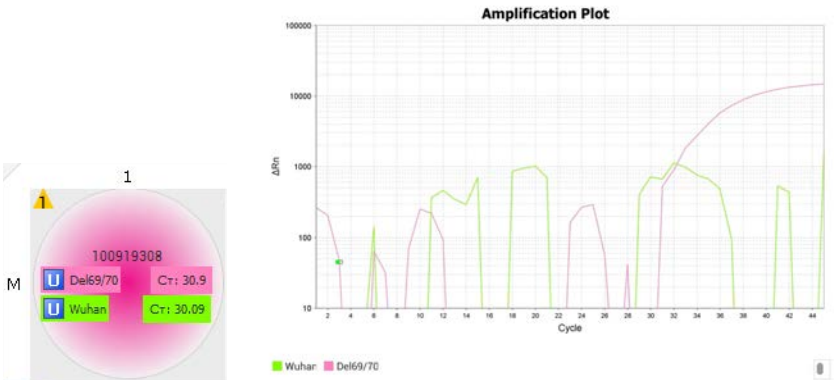

Figure 29. Example of SARS-CoV-2 B.1.1.7 variant (69-70del mutation) positive result interpretation. C_t values of 69-70del and Wuhan probes are 30.9 and 30.09, respectively. Amplification plot curves correspond to 69-70del mutation (pink) and Wuhan sequence (green). Sample was collected and analysed on 8th of April 2021 and its identification was 100919308.

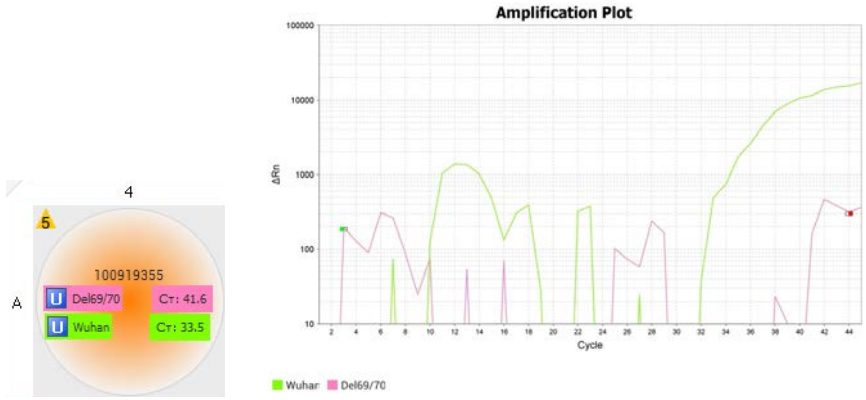

Figure 30. Example of original SARS-CoV-2 (Wuhan sequence) positive result interpretation. C_t values of 69-70del and Wuhan probes are 41.6 and 33.5, respectively. Amplification plot with curves correspond to 69-70del mutation (pink) and Wuhan sequence (green). Sample was collected and analysed on 8th of April 2021 and its identification was 100919355.

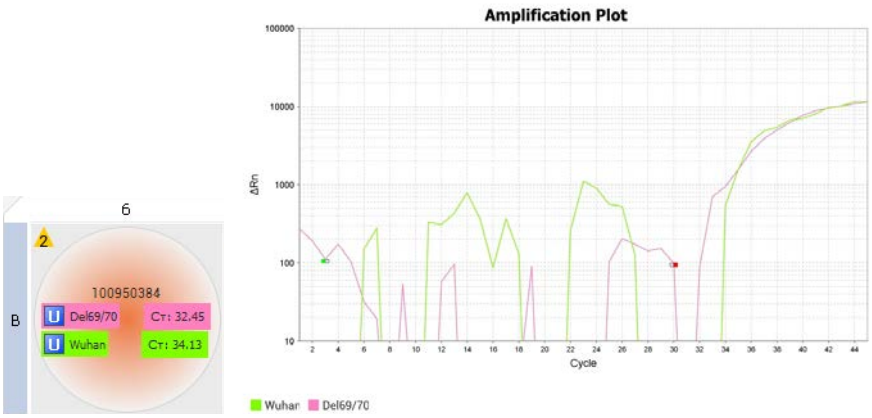

Figure 31. Example of both 69-70del mutation and Wuhan positive result interpretation. C_t values of 69-70del and Wuhan probes are 32.45 and 34.13, respectively. Amplification plot with curves correspond to 69-70del mutation (pink) and Wuhan sequence (green). Sample was collected and analysed on 8th of April 2021 and its identification was 100950384.

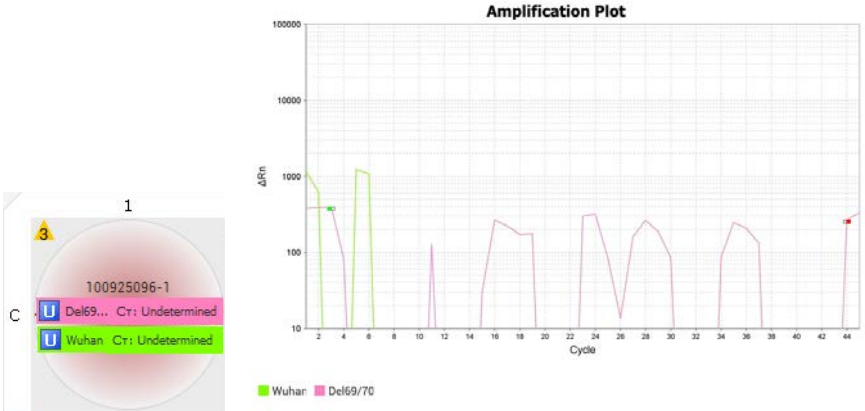

Figure 32. Example of negative result interpretation for of SARS-CoV-2 B.1.1.7 variant. C_t values of 69-70del and Wuhan probes were both undetermined. Amplification plot shows no curves. Sample was collected and analysed on 8th of April 2021 and its identification was 100925096 -1 (10^{-1} diluted).

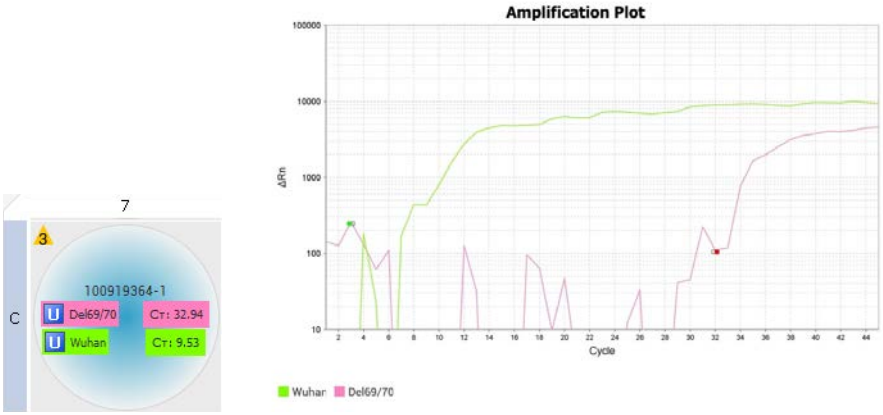

Figure 33.1. Example of false positive result interpretation for original SARS-CoV-2 (Wuhan sequence). C_t values of 69-70del and Wuhan probes are 32.94 and 9.53, respectively. Amplification plot curves correspond to 69-70del mutation (pink) and Wuhan sequence (green). Sample was collected and analysed on 8th of April 2021 and its identification was 100919364 -1 (10^{-1} diluted).

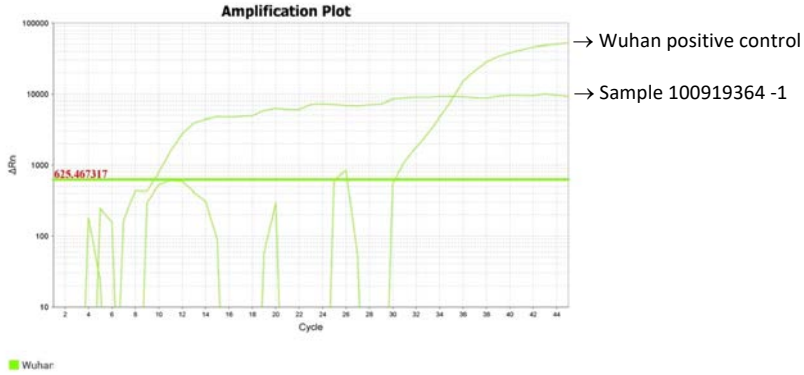

Figure 33.2. Comparison of 100919364 -1 sample curve with original SARS-CoV-2 (Wuhan sequence) positive control, as an example of false-positive result.

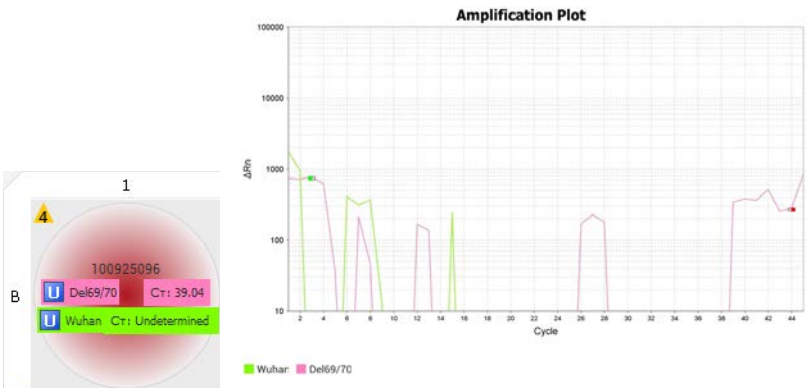

Figure 34. Example of false positive result interpretation for original SARS-CoV-2 (Wuhan sequence). C_t values of 69-70del and Wuhan probes are 39.04 and undetermined, respectively. Amplification plot curves correspond to 69-70del (pink) and Wuhan (green). Sample was collected and analysed on 8th of April 2021 and sample identification is 100925096.

5.4. Monitoring of SARS-CoV-2 variants in wastewater samples

After RT-qPCR conditions for SARS-CoV-2 variants detection optimization and methods calibration were established, real wastewater samples could be analysed to determine the viral concentration of each SARS-CoV-2 variant in every sample. Each wastewater sample was analysed directly and ten-fold diluted to avoid possible PCR inhibitors. The threshold was automatically set by the instrument software in each RT-qPCR reaction. Results were analysed in the thermocycler software and Figure 35 show how they were provided. The C_t values obtained for each sample were compared to the C_t obtained in the SARS-CoV-2 assays performed routinely in the enterprise laboratory, where they analyse targets E, N1 and N2 of SARS-CoV-2). The C_t values were similar in both assays.

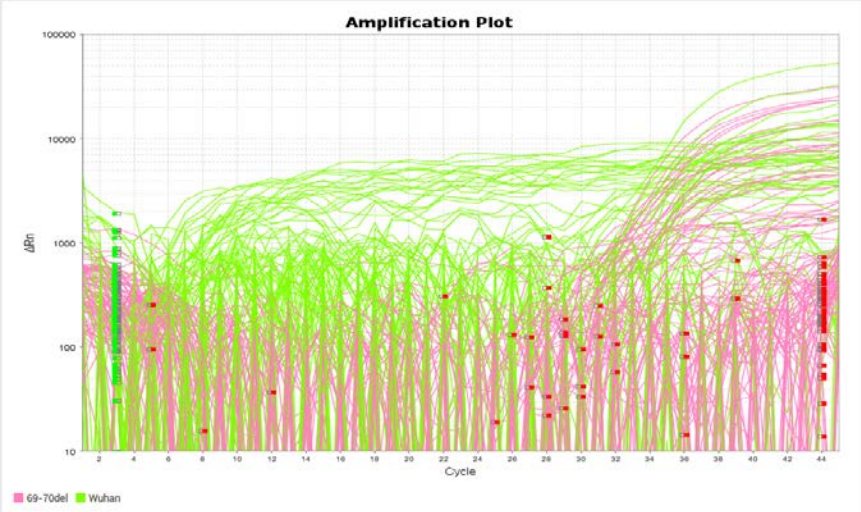

Figure 35. Amplification plot of wastewater samples collected on 8th April 2021 (complete image is shown in Annex 1). Pink curves correspond to samples with 69-70del mutation and green curves corresponds to samples with wild-type sequence. Curves below 1000 ΔRn, approximately, correspond to fluorescence background.

The wastewater samples analysed in this project were collected in the region of Valencia between 31st March to 23rd April. Results of SARS-CoV-2 B.1.1.7 variant quantification are evidenced in Annex 2 and a summary of the results is presented in Table 15. Results of SARS-CoV-2 B.1.351 variant are not presented due to this variant was not detected in the region of Valencia in the period of time analysed.

Table 15. Summary of results of SARS-CoV-2 B.1.1.7 variant detection obtained between 31st March to 23rd April (complete results are shown in Annex 2). A total of 38 geographical points located in the region of Valencia were analysed, where samples had been taken on different days: 2, 3 or 4.

	2 days	**3 days**	**4 days**
Total number of geographical points analysed	3	24	10
Positive results all days analysed	2	12	4
Negative results all days analysed	0	0	0
One negative result in all days analysed	1	5	2
More than one negative result in all days analysed	-	7	4

In this project a total of 117 wastewater samples were analysed by RT-qPCR. The samples were always collected in the same geographical location by enterprise staff members on two to four different days. Thus allowed a SARS-CoV-2 B.1.1.7 variant tracking in different geographical points and evidence the dominant presence of this variant in the region of Valencia in the time period under study. Most of the geographical points analysed were positive all days tested and only a few were negative on the last day analysed. Surprisingly, in some cases in almost a week the viral concentration goes from 10^6 or 10^5 to 0 GU/L, whereas in other cases the concentration goes from 0 to 10^5 GU/L.

6. DISCUSSION

The current pandemic situation caused by SARS-CoV-2 requires to have available methods to detect and quantify SARS-CoV-2 as well as its variants. RT-qPCR is a powerful tool to control the pandemic through positive and asymptomatic cases monitoring. The methods presented in this project to detect SARS-CoV-2 B.1.1.7 and B.1.351 variants in wastewater requires a prior optimization to improve the RT-qPCR specificity and also a standardisation. These methods allow to detect and quantify SARS-CoV-2 B.1.1.7 and B.1.351 variants in samples of wastewater.

6.1. Optimization of the methods

RT-qPCR results obtained with conditions specified by Vogels *et al*. (49) and Yaniv *et al*. (50) to detect SARS-CoV-2 B.1.1.7 and B.1.351 variants, respectively, evidenced a lack of sensitivity (Figures 11 and 12, and Figure 20, respectively). Therefore, the RT-qPCR reactions had to be optimized to reagents and instrument used in the own company's laboratory, as they were designed to use in different laboratory conditions. Tests for optimization were performed based on the literature and the results obtained in each test itself. In these tests, time and temperature of the PCR steps, as well as some master mix reagents were modified.

6.1.1. SARS-CoV-2 B.1.1.7 variant

Firstly, for the detection of B.1.1.7 variant, the reverse transcription step was modified from 10 to 20 minutes to check if any problems in reverse transcriptase enzyme existed. It was evidenced that this step can affect the variability and lack of reproducibility of the RT-PCR reactions (51) and it is also known that the amount of RNA is determinant for an appropriate reaction, as it was reported that small amounts of RNA can inhibit reverse transcriptase activity (52,53). Our results did not evidence any issue in the RT step, as worse results were obtained in comparison to results with initial conditions (10 min). However, in future studies it should be considered to dilute the samples to test for the presence of inhibition. Although RT step seemed to be optimized, the results still evidenced poor sensitivity. Causes of poor sensitivity can be

RNA degradation, RNA ability to form complex structures, DNA contamination, etc. The RNA structure is responsible for its instability, causing it to be more susceptible to hydrolysis than DNA (54). However, its degradation can be avoided by samples storage at -20°C and -80°C for at least one month and by restricting freeze-thaw cycles where possible (55). It is known that 5 freeze-thaw cycles reduce the RNA integrity to 35% approximately (56). Therefore, as maintenance of RNA stability is a key factor to improve PCR sensibility, the samples were always stored at -80°C and its defrosting was limited.

Many evidence reported that PCR reaction specificity shows better results when the annealing temperature is increased, as it allows a perfect match primer-target (57,58). It is established that annealing temperature is the main determinant of reaction specificity and it is also important to avoid false-positive results. If this temperature is too low, nonspecific amplifications will be obtained, whereas excessive high temperatures cause inefficient hybridization of the primers, leading to poor yields. Stringency improvements in the results are obtained with annealing temperature increase, but always considering the primers melting temperature (T_m) (59). For this reason, most of the tests conducted in this project to optimize the detection methods focused on modifying the temperature of annealing and extension step (as both take place in the same step). The initial temperature of this step was 55°C, as described in Vogels *et al.* protocol (49). The tests performed with 57°C, 60°C and 63°C in annealing and extension step evidenced significant improvements when the temperature was 60°C. Nevertheless, amplification plots obtained after modification of annealing and extension temperature showed that further improvements were required, as curves obtained have a shaky appearance. Annealing time from 40 seconds to 1 minute has been established as enough to allow primer hybridization with the complementary target, whereas extension time depends upon the synthesis rate of DNA polymerase and amplicon length (41). As DNA polymerase used in our assays differed from Vogels *et al.* protocol (49), increasing time extension from 30 to 45 seconds allowed us to improve the efficiency of the reaction. Extension time to 1 minute was also tested but it did not show any improvements.

After completion of reverse transcription, a step prior to basic PCR is important for initial DNA denaturation, DNA polymerase activation, and reverse transcriptase inactivation (60). Specifically, deactivation of the reverse transcriptase before cDNA amplification is pivotal, as after reverse transcription takes place the residual reverse transcriptase enzyme can add nucleotides to the primers and can enhance its dimerization. As a consequence, primers cannot anneal with the complementary target and DNA amplification results inhibited (60). Therefore, if some residual reverse transcriptase activity is remaining, the efficiency of the amplification reaction would be considerably reduced. Therefore, the following optimization consisted of modifying the time of the step prior to general PCR from 1 to 2 minutes. No improvements were obtained in our results after time modification, suggesting the absence of residual reverse transcriptase activity.

After steps of RT-PCR reaction were already optimized, modifications of PCR reagents master mix were tested to check if we were able to obtain any improvements at this level. The unique reagent with the possibility to be modified was 5-carboxy-X-rhodamine (ROX). It is a passive reference dye whose fluorescence does not change during the RT-qPCR reaction and it normalizes the fluorescent reporter signal in RT-qPCR. It is usually used as an internal reference, allowing to identify non-PCR related fluctuations in fluorescence, such as pipetting errors, well-to-well variations or instrument limitations, to decrease nonspecific fluorescence (background) and provide a stable fluorescence baseline. Furthermore, its emission spectrum differs completely from fluorescent dyes attached to the probes used in RT-qPCR and several protocols emphasise its usage (61,62). A study by Wang, Becker and Mesa (63) determined that a wide concentration range of ROX can be used for RT-qPCR fluorescence normalization and each chemistry, such as TaqMan or SYBR green, should determine the best ROX concentration to decrease variation in the PCR reproducibility. In our case, different dilutions of ROX were tested and the results indicated that ROX no diluted was the best condition for SARS-CoV-2 B.1.1.7 variant detection through RT-qPCR using TaqMan probes.

6.1.2. SARS-CoV-2 B.1.351 variant

The RT-qPCR conditions tested to detect SARS-CoV-2 B.1.351 variant were similar to SARS-CoV-2 B.1.1.7 variant and the master mix used was the same (TaKaraBio Inc.). Therefore, the optimization was more specific and could be performed in less time. ROX was directly tested undiluted, as it showed significant improvement in B.1.1.7 variant method optimization. The results with initial conditions (without any optimization) evidenced some shakiness in the plateau phase of the amplification curve. It was though that not enough time for appropriate extension was responsible for it, and annealing and extension time was increased. This increase significantly improved the amplification curves. Therefore, these conditions were considered as already optimized.

6.2. Calibration of the methods

After the RT-qPCR methodologies to detect both variants were completely optimized, it was necessary to calibrate them through the standard curve method to allow quantification of the SARS-CoV-2 B.1.1.7 and B.1.351 variants. The calibration was based on measuring different concentrations (ten-folded serial dilutions) of reference material (plasmids of known concentration) and plotted them against the C_t value obtained in the RT-qPCR, as explained in the results section. This enables to obtain a regression line between the known RNA concentrations and C_t values. The straight-line equation obtained can be used to extrapolate the samples concentrations according to its C_t value obtained in the RT-qPCR assay. It is important to consider that the reliability of RT-qPCR results relies upon the standardisation of measurements (64). The importance of the method standardisation also relies upon the measure of efficiency, defined as the fraction of target molecules copies in each PCR cycle. Therefore, 100% efficiency implies that in every cycle of PCR the whole amount of DNA become duplicated. It is important to consider that a perfect doubling of amplicon in each cycle is highly uncommon due to many reasons, such as formation of secondary structures by the primers, presence of inhibitors in the sample matrix, reagents characteristics, etc. (65). The efficiency in the standard curve method is indicated by the slope parameter (calculations in Annex 3) and, according to the ISO 15216-1:2017(E), it

should be between 90-110%, which is achieved with slope values between -3.10 and -3.60. Moreover, r^2 values of <0,980 shall not be used for calculations. In our assays, the slope and efficiency parameters were -3.28 and 1.02 for SARS-CoV-2 B.1.1.7 variant, and -3.58 and 0.90 for SARS-CoV-2 B.1.351 variant, respectively. These parameters indicate that both reaction efficiency was adequate, as well as r^2 parameters. It was also reported that the use of different thermocycler has an impact on the reaction efficiency (65). Therefore, the RT-qPCR assays were always performed in the same instrument. The standard curve method is commonly accepted and is the most reliable method to assess the efficiency of PCR assays. Moreover, the reaction specificity and sensitivity are also important parameters to determine in new assays, referring to the percentage of negative and positive results correctly assessed, respectively. High percentages are desired to avoid false-negative and false-positive results (65), which were achieved with the method optimizations described in results section.

6.3. Monitoring of SARS-CoV-2 variants in wastewater samples

Once the detection methods were optimized and standardized to detect B.1.1.7 and B.1.351 variants of SARS-CoV-2, real wastewater samples were analysed. However, only results for SARS-CoV-2 B.1.1.7 variant are presented because there were no positive cases of SARS-CoV-2 B.1.351 variant during the samples collection period (31st March-23rd April).

In Figure 35 it is shown the results of SARS-CoV-2 B.1.1.7 variant of all samples analysed on one day randomly selected (8th March 2021). It evidences false-positive results identified by green irregular and non-exponential curves with very low C_t values. These curves correspond to the Wuhan sequence amplification and were obtained in most of the tests performed. It was decided to not use the Wuhan probe in the B.1.1.7 variant detection assays and to detect only the presence of B.1.1.7 variant. Initially, the idea was to compare the concentration of SARS-CoV-2 original and B.1.1.7 variant in samples analysed, and to determine the variant frequency at the target locus. However, as the Wuhan probe did not work properly, it was not used in the assays. Moreover, as other routinely assays performed in the company's laboratory already analysed the presence of original SARS-CoV-2 for a set of specific genes, such

as N1, N2 and E, its quantification was already assessed. In another hand, it was decided to analyse only 69-70del mutation to detect the SARS-CoV-2 B.1.1.7 variant as a previous study reported its presence in 98.7% of SARS-CoV-2 sequences analysed. However, it is important to remark that it was also detected in 2.5% sequences of other variants (66). In future assays, it should be considered to detect other mutations that could aid to discriminate more precisely between different SARS-CoV-2 variants.

Samples collected in the same geographical location through several days evidenced the dominant presence of SARS-CoV-2 B.1.1.7 variant in the region of Valencia from 31st March to 23rd April. These data were transferred to the government authorities and they were of great help to decide social restrictions to be applied. The more important about sewage analysis is that SARS-CoV-2 RNA can be detected in human faeces a few days to a week before the onset of symptoms in the people who became infected (67). Therefore, the delay between initial infection, symptoms to be developed and samples to be collected is saved in wastewater RT-qPCR analysis. Furthermore, it allows virus detection in asymptomatic patients. This is extremely helpful for authorities, as it allows them to act in advance to decide restrictions to be applied (or relaxed) in order to limit the virus spreading. The cumulative incidence (per 100,000 inhabitants) in the Valencian Community between 31st March to 23rd April was quite low (68) and the results presented in this project corroborate it. Surprisingly, in the Valencian Community, it was able to reduce the positive cases from 11064 on 23rd January (being the peak of positive cases) to 530 on 23rd February and to 141 on 23rd May (68) (Annex 4). Nevertheless, even though the positive cases were maintained in low levels, the viral load quantification revealed that levels of SARS-CoV-2 B.1.1.7 variant were still concerning in that period of time. The authorities decided to be cautious and maintained strict social restrictions more time, as this variant is highly transmissible.

It is remarkable that during the SARS-CoV-1 outbreak (2004), detection of SARS-CoV-1 in wastewater samples was already performed (69) and that previously to SARS-CoV-2 emergence, detection of pathogens in wastewater was already being performed, such as enterovirus, adenovirus, hepatitis virus, Norwalk virus, etc. (70). Furthermore, a

recent study was performed in the European Union to determine the illicit drug use by wastewater analysis (71). All of this highlights the important value of analysing wastewater. In the case of SARS-CoV-2 tracking and its variants, it was greatly reported the usefulness and potential predictive of its detection in wastewater in several countries, such as in the USA (72), Germany (73), Italy (74), Netherlands (75), Australia (76), etc. In addition, previous studies had demonstrated the sensitivity of RT-qPCR to detect SARS-CoV-2 in wastewater samples. For example, SARS-CoV-2 was consistently detected at beginning of the pandemic, when less than a hundred positive cases were identified in the whole region of Valencia (77). Furthermore, previous studies have revealed that the peaks in viral load present in wastewater were in line with new hospitalizations due to COVID-19 (78) and that analysing specific regions, such as nursing homes, could aid to identify isolated cases or outbreaks of SARS-CoV-2 infection (79). In this way, keeping in surveillance the nursing homes was helpful to control the pandemic and avoid further deaths, as elderly people are considered a group at risk for the COVID-19.

However, it is important to remark that the study of wastewater samples implies some challenges. The assays are required to be highly sensitive due to the viral concentration in wastewater samples is very diluted in comparison to clinical samples, and there is also a high probability that RT-qPCR inhibitors are present in wastewater (66). The best option to detect SARS-CoV-2 variants in wastewater samples is sequencing the entire genome or specific *loci*, as it ensures the identification of all mutations that characterize each variant. Nevertheless, sequencing is a time-consuming technique that requires specific equipment and professionals to interpret the huge number of results obtained. It also implies high financial costs, which are not affordable for all laboratories. While the RT-qPCR technique is widely available due to its lower costs and time required, and it also allows to quantify the abundance of the target (66).

7. CONCLUSION

Before the SARS-CoV-2 outbreak, wastewater analysis was already being performed in laboratories worldwide to detect pathogens presence or to study the population's health. However, the COVID-19 pandemic has greatly elucidated its usefulness. Analysing SARS-CoV-2 and its variants in wastewater samples collected from different regions or specific zones, such as hospitals or nursing homes, results in an early warning system for COVID-19 incidence. It allows to establish SARS-CoV-2 variants frequencies and dynamics within a community and to act in advance to avoid further infections and infection outbreaks. This was of great help to the authorities in applying social restrictions to limit the virus spreading and, in the case of VOCs, was even more helpful as they are characterised by higher infectiousness. Although the analysis of SARS-CoV-2 and its variants in wastewater by RT-qPCR implies some limitations, this analysis had made it possible to track the virus spreading more accurately than clinical testing of patients, as wastewater analysis avoids the delay between clinical symptoms development of the infected patient and sample collection, and also allows the detection of asymptomatic cases. Specifically, methodologies presented in this project were very useful to track SARS-CoV-2 B.1.1.7 and B.1.351 variants in wastewater samples from different geographical locations. Nevertheless, for a more accurate variants monitoring, more than one mutation should be detected in each variant assay.

In addition, if wastewater analysis is imposed as a routine analysis in laboratories worldwide, it will allow detecting possible re-emergence of SARS-CoV-2 in the future, as well as new variants outbreak in the near future. This is of great importance as new variants could compromise the vaccine's efficacy against SARS-CoV-2, shattering all the effort made in the last months to control the pandemic. In addition, the emergence of new variants calls into question if the current vaccines will provide long-term immunity against infection. Furthermore, as population vaccination quickly move forward and VOCs continue spreading, the evolutionary pressure for viral variants to be selected ratchets up (80). For all these reasons, it is crucial to implement an intensive surveillance of viral infection, specifically of new variants, and wastewater analysis by RT-qPCR is a very potential candidate for it. This will be essential to achieve the pandemic ends. In addition, it has been proposed to keep the wastewater analysis

after the COVID-19 pandemic as a system to study and monitor the population's health, known as wastewater-based epidemiology (WBE) (81).

8. BIBLIOGRAPHY

1. Kumar Mishra S, Tripathi T. One year update on the COVID-19 pandemic: Where are we now? Acta Tropica. 2020.
2. Santos CF. Reflections about the impact of the SARS-CoV-2/ COVID-19 pandemic on mental health. Vol. 42, Brazilian Journal of Psychiatry. Associacao Brasileira de Psiquiatria; 2020. p. 329.
3. Al-Qaaneh AM, Alshammari T, Aldahhan R, Aldossary H, Alkhalifah ZA, Borgio JF. Genome composition and genetic characterization of SARS-CoV-2. Saudi Journal of Biological Sciences. 2021 Mar 1;28(3):1978–89.
4. Naqvi AAT, Fatima K, Mohammad T, Fatima U, Singh IK, Singh A, et al. Insights into SARS-CoV-2 genome, structure, evolution, pathogenesis and therapies: Structural genomics approach. Biochimica et Biophysica Acta - Molecular Basis of Disease. 2020 Oct 1;1866(10):165878.
5. Al-Qaaneh AM, Alshammari T, Aldahhan R, Aldossary H, Alkhalifah ZA, Borgio JF. Genome composition and genetic characterization of SARS-CoV-2. Vol. 28, Saudi Journal of Biological Sciences. Elsevier B.V.; 2021. p. 1978–89.
6. Arya R, Kumari S, Pandey B, Mistry H, Bihani SC, Das A, et al. Structural insights into SARS-CoV-2 proteins. Vol. 433, Journal of Molecular Biology. Academic Press; 2021. p. 166725.
7. Kadam SB, Sukhramani GS, Bishnoi P, Pable AA, Barvkar VT. SARS-CoV-2, the pandemic coronavirus: Molecular and structural insights. Journal of Basic Microbiology. 2021 Mar 1;61(3):180–202.
8. Xu H, Zhong L, Deng J, Peng J, Dan H, Zeng X, et al. High expression of ACE2 receptor of 2019-nCoV on the epithelial cells of oral mucosa. International Journal of Oral Science. 2020 Dec 1;12(1).
9. Yao H, Song Y, Chen Y, Wu N, Xu J, Sun C, et al. Molecular Architecture of the SARS-CoV-2 Virus. Cell. 2020 Oct 29;183(3):730–8.
10. V'kovski P, Kratzel A, Steiner S, Stalder H, Thiel V. Coronavirus biology and replication: implications for SARS-CoV-2. Vol. 19, Nature Reviews Microbiology. Nature Research; 2021. p. 155–70.
11. Meyerowitz EA, Richterman A, Gandhi RT, Sax PE. Transmission of SARS-CoV-2: A Review of Viral, Host, and Environmental Factors. Annals of internal medicine. 2021 Jan 1;174(1):69–79.
12. Byambasuren O, Cardona M, Bell K, Clark J, McLaws ML, Glasziou P. Estimating the extent of asymptomatic COVID-19 and its potential for community transmission: Systematic review and meta-analysis. Journal of the Association of Medical Microbiology and Infectious Disease Canada. 2020 Dec 1;5(4):223–34.
13. Jacques FH, Apedaile E. Immunopathogenesis of COVID-19: Summary and Possible Interventions. Frontiers in Immunology. 2020 Sep 17;11.
14. Bordallo B, Bellas M, Cortez AF, Vieira M, Pinheiro M. Severe COVID-19: What have we learned with the immunopathogenesis? Advances in Rheumatology. 2020 Sep 22;60(1).
15. Zhou D, Dejnirattisai W, Supasa P, Liu C, Mentzer AJ, Ginn HM, et al. Evidence of escape of SARS-CoV-2 variant B.1.351 from natural and vaccine-induced sera. Cell. 2021 Apr 29;184(9):2348–61.
16. Russell RL, Pelka P, Mark BL. Frontrunners in the race to develop a SARS-CoV-2 vaccine. Canadian Journal of Microbiology. 2021;67(3):189–212.
17. Duffy S. Why are RNA virus mutation rates so damn high? PLoS Biology. 2018 Aug 13;16(8).
18. SARS-CoV-2 variants of concern as of 3 June 2021 [Internet]. [cited 2021 Jun 5]. Available from: https://www.ecdc.europa.eu/en/covid-19/variants-concern
19. Buenestado-Serrano S, Recio R, Sola Campoy PJ, Catalán P, Folgueira MD, Villa J, et al. First confirmation of importation and transmission in Spain of the newly identified SARS-CoV-2 B.1.1.7 variant. Enfermedades Infecciosas y Microbiologia Clinica. 2021.
20. Health England P. Investigation of novel SARS-CoV-2 variant: Variant of Concern 202012/01.
21. Tang JW, Tambyah PA, Hui DS. Emergence of a new SARS-CoV-2 variant in the UK. Vol. 82, Journal of Infection. W.B. Saunders Ltd; 2021. p. e27–8.

22. Liu Y, Liu J, Plante KS, Plante JA, Xie X, Zhang X, et al. The N501Y spike substitution enhances SARS-CoV-2 transmission. bioRxiv. 2021.
23. Kemp SA, Meng B, Ferriera IA, Datir R, Harvey WT, Papa G, et al. Recurrent emergence and transmission of a SARS-CoV-2 spike deletion H69/V70. bioRxiv. 2021 Mar 8.
24. Davies NG, Jarvis CI, van Zandvoort K, Clifford S, Sun FY, Funk S, et al. Increased mortality in community-tested cases of SARS-CoV-2 lineage B.1.1.7. Nature. 2021 May 13;593(7858):270–4.
25. Challen R, Brooks-Pollock E, Read JM, Dyson L, Tsaneva-Atanasova K, Danon L. Risk of mortality in patients infected with SARS-CoV-2 variant of concern 202012/1: Matched cohort study. BMJ. 2021 Mar 9;372.
26. Shen X, Tang H, McDanal C, Wagh K, Fischer W, Theiler J, et al. SARS-CoV-2 variant B.1.1.7 is susceptible to neutralizing antibodies elicited by ancestral spike vaccines. Cell Host and Microbe. 2021 Apr 14;29(4):529–39.
27. Emary KRW, Golubchik T, Aley PK, Ariani C v., Angus BJ, Bibi S, et al. Efficacy of ChAdOx1 nCoV-19 (AZD1222) Vaccine Against SARS-CoV-2 VOC 202012/01 (B.1.1.7). SSRN Electronic Journal. 2021 Feb 7.
28. Lineage B.1.1.7 [Internet]. Pango lineages. [cited 2021 Jun 5]. Available from: https://cov-lineages.org/global_report_B.1.1.7.html
29. Ecdc. SARS-CoV-2 - increased circulation of variants of concern and vaccine rollout in the EU/EEA - 14th update [Internet]. [cited 2021 Jun 6]. Available from: https://www.ecdc.europa.eu/en/covid-19/timeline-ecdc-response.This
30. Lineage B.1.351 [Internet]. Pango lineages. [cited 2021 Jun 6]. Available from: https://cov-lineages.org/global_report_B.1.351.html
31. Actualización de la situación epidemiológica de la variante B.1.1.7 de SARS-CoV-2 y otras variantes de interés. Ministerio de Sanidad. Centro de Coordinación de Alertas y Emergencias Sanitarias. 2021.
32. Tegally H, Wilkinson E, Giovanetti M, Iranzadeh A, Fonseca V, Giandhari J, et al. Emergence and rapid spread of a new severe acute respiratory syndrome-related coronavirus 2 (SARS-CoV-2) lineage with multiple spike mutations in South Africa. medRxiv. 2020 Dec 22;10.
33. Zhou D, Dejnirattisai W, Supasa P, Liu C, Mentzer AJ, Ginn HM, et al. Evidence of escape of SARS-CoV-2 variant B.1.351 from natural and vaccine-induced sera. Cell. 2021 Apr 29;184(9):2348-2361.
34. Zhou D, Dejnirattisai W, Supasa P, Liu C, Mentzer AJ, Ginn HM, et al. Evidence of escape of SARS-CoV-2 variant B.1.351 from natural and vaccine-induced sera. Cell. 2021 Apr 29;184(9):2348–61.
35. Funk T, Pharris A, Spiteri G, Bundle N, Melidou A, Carr M, et al. Characteristics of SARS-CoV-2 variants of concern B.1.1.7, B.1.351 or P.1: data from seven EU/EEA countries, weeks 38/2020 to 10/2021. Eurosurveillance. 2021 Feb 1;26(16):2100348.
36. Fontanet A, Autran B, Lina B, Kieny MP, Karim SSA, Sridhar D. SARS-CoV-2 variants and ending the COVID-19 pandemic. Vol. 397, The Lancet. Elsevier B.V.; 2021. p. 952–4.
37. Diagnostic testing for SARS-CoV-2 [Internet]. WHO. [cited 2021 Jun 6]. Available from: https://www.who.int/publications/i/item/diagnostic-testing-for-sars-cov-2
38. Hernández-Pérez JM, Martín-González E, Pino-Yanes M. Strengths and weaknesses of the diagnostic tests for SARS-CoV-2 infection. Medicina Clínica (English Edition). 2020 Nov;155(10):464–5.
39. Bruno R, Mondelli M, Brunetti E, Matteo A di, Seminari E, Maiocchi L, et al. Performance of VivaDiag COVID-19 IgM/IgG Rapid Test is inadequate for diagnosis of COVID-19 in acute patients referring to emergency room department. Vol. 92, Journal of Medical Virology. John Wiley and Sons Inc; 2020. p. 1724–7.
40. Sullivan D, Fahey B, Titus D. Fast PCR: General Considerations for Minimizing Run Times and Maximizing Throughput. 2006.
41. Real-time PCR handbook [Internet]. Life technologies. [cited 2021 Jun 6]. Available from: https://www.gene-quantification.de/real-time-pcr-handbook-life-technologies-update-flr.pdf
42. Wurtzer S, Marechal V, Mouchel J, Maday Y, Teyssou R, Richard E, et al. Evaluation of lockdown impact on SARS-CoV-2 dynamics through viral genome quantification in Paris wastewaters. medRxiv. 2020 May 6.
43. Jahn K, Dreifuss D, Topolsky I, Kull A, Ganesanandamoorthy P, Fernandez-Cassi X, et al. Detection of SARS-CoV-2 variants in Switzerland by genomic analysis of wastewater samples. medRxiv. 2021 Jan 9.

44. Gupta S, Parker J, Smits S, Underwood J, Dolwani S. Persistent viral shedding of SARS-CoV-2 in faeces – a rapid review. Vol. 22, Colorectal Disease. Blackwell Publishing Ltd; 2020. p. 611–20.
45. Rimoldi SG, Stefani F, Gigantiello A, Polesello S, Comandatore F, Mileto D, et al. Presence and infectivity of SARS-CoV-2 virus in wastewaters and rivers. Science of the Total Environment. 2020 Nov 20;744.
46. Water, sanitation, hygiene, and waste management for SARS-CoV-2, the virus that causes COVID-19 [Internet]. WHO. 2020 [cited 2021 Jun 6]. Available from: https://www.who.int/publications/i/item/WHO-2019-nCoV-IPC-WASH-2020.4
47. Zang R, Castro MFG, McCune BT, Zeng Q, Rothlauf PW, Sonnek NM, et al. TMPRSS2 and TMPRSS4 promote SARS-CoV-2 infection of human small intestinal enterocytes. Science Immunology. 2020 May 13;5(47).
48. Randazzo W, Truchado P, Cuevas-Ferrando E, Simón P, Allende A, Sánchez G. SARS-CoV-2 RNA in wastewater anticipated COVID-19 occurrence in a low prevalence area. Water Research. 2020 Aug 15;181.
49. Vogels CBF, Alpert T, Breban M, Fauver JR, Grubaugh ND. Multiplexed RT-qPCR to screen for SARS-COV-2 B.1.1.7 variants: Preliminary results. Virological.org. 2021.
50. Yaniv K, Ozer E, Plotkin N, Suresh Bhandarkar N, Kushmaro A. RT-qPCR assay for detection of British (B.1.1.7) and South Africa (B.1.351) variants of SARS-CoV-2. medRxiv. 2021.
51. Bustin SA, Benes V, Nolan T, Pfaffl MW. Quantitative real-time RT-PCR - A perspective. Vol. 34, Journal of Molecular Endocrinology. BioScientifica; 2005. p. 597–601.
52. Levesque-Sergerie JP, Duquette M, Thibault C, Delbecchi L, Bissonnette N. Detection limits of several commercial reverse transcriptase enzymes: Impact on the low- and high-abundance transcript levels assessed by quantitative RT-PCR. BMC Molecular Biology. 2007 Oct 22;8(1):1–18.
53. Suslov O, Steindler DA. PCR inhibition by reverse transcriptase leads to an overestimation of amplification efficiency. Nucleic Acids Research. 2005;33(20):e181.
54. Fordyce SL, Kampmann ML, van Doorn NL, Gilbert MTP. Long-term RNA persistence in postmortem contexts. Vol. 4, Investigative Genetics. BioMed Central; 2013. p. 1–7.
55. Wu J, Kim L, Huang C, Anekella B. Stability of Extracted RNA at Various Storage Temperatures and through Multiple Freeze-Thaw Cycles. Arlington: SeraCare Life Sciences; 2011.
56. Yu K, Xing J, Zhang J, Zhao R, Zhang Y, Zhao L. Effect of multiple cycles of freeze–thawing on the RNA quality of lung cancer tissues. Cell and Tissue Banking. 2017 Sep 1;18(3):433–40.
57. Wu DY, Ugozzoli L, Pal BK, Qian J, Wallace RB. The Effect of Temperature and Oligonucleotide Primer Length on the Specificity and Efficiency of Amplification by the Polymerase Chain Reaction. DNA and Cell Biology. 1991 Mar 25;10(3):233–8.
58. Rychlik W, Spencer WJ, Rhoads RE. Optimization of the annealing temperature for DNA amplification in vitro. Nucleic Acids Research. 1990 Nov 21;18(21):6409–12.
59. Starčič Erjavec M. Annealing Temperature of 55°C and Specificity of Primer Binding in PCR Reactions. In: Synthetic Biology - New Interdisciplinary Science. IntechOpen; 2019.
60. Chumakov KM. Reverse transcriptase can inhibit PCR and stimulate primer-dimer formation. PCR Methods and Applications. 1994;4(1):62–4.
61. Normalization of Real-Time PCR Fluorescence Data with ROX Passive Reference Dye [Internet]. BioRad. [cited 2021 Jun 7]. Available from: https://www.bio-rad.com/es-es/applications-technologies/normalization-real-time-pcr-fluorescence-data-with-rox-passive-reference-dye?ID=MW472W15
62. ThermoFisher. ROX passive reference dye for troubleshooting real-time PCR.
63. Wang G, Becker E, Mesa C. Optimization of 6-carboxy-X-rhodamine concentration for real-time polymerase chain reaction using molecular beacon chemistry. Canadian Journal of Microbiology. 2007 Mar;53(3):391–7.
64. Sanders R, Bustin S, Huggett J, Mason D. Improving the standardization of mRNA measurement by RT-qPCR. Biomolecular Detection and Quantification. 2018 May 1;15:13–7.
65. Svec D, Tichopad A, Novosadova V, Pfaffl MW, Kubista M. How good is a PCR efficiency estimate: Recommendations for precise and robust qPCR efficiency assessments. Biomolecular Detection and Quantification. 2015 Mar 1;3:9–16.
66. Lee WL, Mcelroy KA, Armas F, Imakaev M, Gu X, Duvallet C, et al. Quantitative detection of SARS-CoV-2 B.1.1.7 variant in wastewater by allele-specific RT-qPCR. medRxiv. 2021 Mar 29;

67. Chen Y, Chen L, Deng Q, Zhang G, Wu K, Ni L, et al. The presence of SARS-CoV-2 RNA in the feces of COVID-19 patients. Journal of Medical Virology. 2020 Jul 1;92(7):833–40.
68. Información estadística sobre coronavirus en la Comunidad Valenciana - Conselleria de Sanidad Universal y Salud Pública [Internet]. [cited 2021 Jun 7]. Available from: http://coronavirus.san.gva.es/es/estadisticas
69. Wang XW, Li J, Guo T, Zhen B, Kong Q, Yi B, et al. Concentration and detection of SARS coronavirus in sewage from Xiao Tang Shan hospital and the 309th Hospital of the Chinese People's Liberation Army. Water Science and Technology. 2005 Oct 1;52(8):213–21.
70. Wong MVM, Hashsham SA, Gulari E, Rouillard JM, Aw TG, Rose JB. Detection and characterization of human pathogenic viruses circulating in community wastewater using multi target microarrays and polymerase chain reaction. Journal of Water and Health. 2013 Dec 1;11(4):659–70.
71. European Monitoring Centre for Drugs and Drug Addiction. Wastewater analysis and drugs: a European multi-city study [Internet]. [cited 2021 Jun 7]. Available from: www.emcdda.europa.eu/
72. Peccia J, Zulli A, Brackney DE, Grubaugh ND, Kaplan EH, Casanovas-Massana A, et al. Measurement of SARS-CoV-2 RNA in wastewater tracks community infection dynamics. Nature Biotechnology. 2020 Oct 1;38(10):1164–7.
73. Agrawal S, Orschler L, Lackner S. Long-term monitoring of SARS-CoV-2 RNA in wastewater of the Frankfurt metropolitan area in Southern Germany. Scientific reports. 2021 Mar 8;11(1):5372.
74. la Rosa G, Iaconelli M, Mancini P, Bonanno Ferraro G, Veneri C, Bonadonna L, et al. First detection of SARS-CoV-2 in untreated wastewaters in Italy. Science of the Total Environment. 2020 Sep 20;736.
75. Medema G, Heijnen L, Elsinga G, Italiaander R, Brouwer A. Presence of SARS-Coronavirus-2 RNA in Sewage and Correlation with Reported COVID-19 Prevalence in the Early Stage of the Epidemic in the Netherlands. Environmental Science and Technology Letters. 2020 Jul 14;7(7):511–6.
76. Ahmed W, Angel N, Edson J, Bibby K, Bivins A, O'Brien JW, et al. First confirmed detection of SARS-CoV-2 in untreated wastewater in Australia: A proof of concept for the wastewater surveillance of COVID-19 in the community. Science of the Total Environment. 2020 Aug 1;728:138764.
77. Randazzo W, Cuevas-Ferrando E, Sanjuán R, Domingo-Calap P, Sánchez G. Metropolitan wastewater analysis for COVID-19 epidemiological surveillance. International Journal of Hygiene and Environmental Health. 2020 Sep 1;230:113621.
78. Saguti F, Magnil E, Enache L, Churqui MP, Johansson A, Lumley D, et al. Surveillance of wastewater revealed peaks of SARS-CoV-2 preceding those of hospitalized patients with COVID-19. Water Research. 2021 Feb 1;189:116620.
79. Dav L, Seguí R, Botija P, Beltrán MJ, Albert E, Torres I, et al. Early detection of SARS-CoV-2 infection cases or outbreaks at nursing homes by targeted wastewater tracking. Clinical Microbiology and Infection. 2021.
80. Gupta RK. Will SARS-CoV-2 variants of concern affect the promise of vaccines? Nature Reviews Immunology. 2021 Apr 29;21(6):340–1.
81. Aguiar-Oliveira M de L, Campos A, Matos AR, Rigotto C, Sotero-Martins A, Teixeira PFP, et al. Wastewater-based epidemiology (Wbe) and viral detection in polluted surface water: A valuable tool for covid-19 surveillance—a brief review. Vol. 17, International Journal of Environmental Research and Public Health. MDPI AG; 2020. p. 1–19.

9. ANNEX

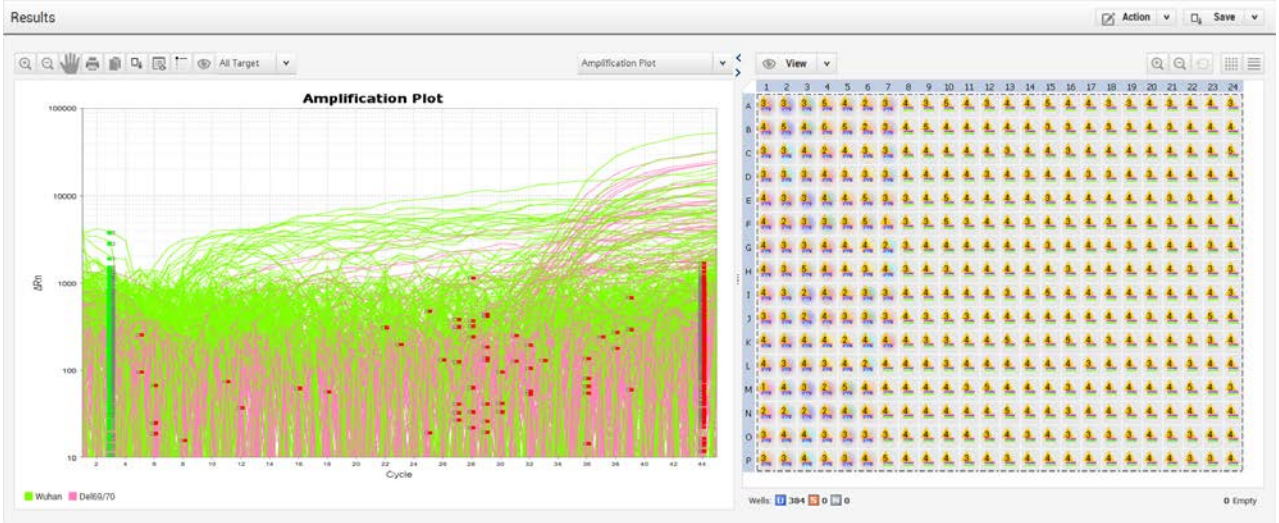

Annex 1. Screenshot of RT-qPCR results provided by the thermocycler software. 384 wells are shown on the right. The wells containing sample are indicated in different colour. It is possible to indicate which sample was deposited in each well. The amplification plot of all samples is shown on the left, where each curve represents one sample. Samples shown were collected and analysed on 8th of April 2021.

Annex 2. Tables of results in 69-70del mutation analysed from 31st March to 23rd April. The results are presented according to days on which samples were taken and the locator groups samples taken in the same location but in different days (Tables 1-8).

Table 1. Results of samples collected from 31st of March to 21st of April 2021.

Locator	Identification number	Days analysed	69-70del results	Concentration (GU/L)
P064	100915382	31/03/2021	+	11161
	100919191	07/04/2021	+	541938
	100920458	14/04/2021	+	747222
	100921944	21/04/2021	+	--
P065	100915384	31/03/2021	-	--
	100919200	07/04/2021	+	133076
	100920495	14/04/2021	+	82557
	100921897	21/04/2021	+	--
P021	100915386	31/03/2021	+	20130
	100919193	07/04/2021	+	30893
	100921877	21/04/2021	+	--
E098	100915783	31/03/2021	+	1982872
	100919163	07/04/2021	+	86715
	100920615	14/04/2021	+	12240925
E112	100915785	31/03/2021	+	43197
	100919161	07/04/2021	+	69754
	100920601	14/04/2021	+	963801

E094	100915790	31/03/2021	+	125807
	100919165	07/04/2021	+	105554
	100920609	14/04/2021	+	780747

Table 2. Results of samples collected from 31st of March to 23rd of April 2021.

Locator	Identification number	Days analysed	69-70del results	Concentration (GU/L)
P094	100928523	31/03/2021	+	47326
	100919478	09/04/2021	+	18277
	100920813	16/04/2021	+	365756
	100922097	23/04/2021	+	--
P095	100928524	31/03/2021	+	1723097
	100919480	09/04/2021	+	59352
	100920807	16/04/2021	+	304727
P096	100928525	31/03/2021	+	65367
	100919486	09/04/2021	+	19990
	100920844	16/04/2021	+	136867
P097	100928526	31/03/2021	+	795963
	100919468	09/04/2021	+	211885
	100920838	16/04/2021	+	498148
P098	100928527	31/03/2021	+	1620435
	100919495	09/04/2021	+	214511
	100920833	16/04/2021	+	614944
	100922112	23/04/2021	+	--

Table 3. Results of samples collected from 1st to 16th of April 2021.

Locator	Identification number	Days analysed	69-70del results	Concentration (GU/L)
P149	100918131	01/04/2021	+	1010572
	100919489	09/04/2021	+	23658
	100920748	16/04/2021	+	199966
P127	100918132	01/04/2021	-	--
	100919517	09/04/2021	+	16307
	100920840	16/04/2021	+	553474
P047	100918180	01/04/2021	+	408521
	100919457	09/04/2021	+	808642
	100920805	16/04/2021	+	324604

Table 4. Results of samples collected from 1st to 15th of April 2021.

Locator	Identification number	Days analysed	69-70del results	Concentration (GU/L)
P013	100918097	01/04/2021	-	--
	100919364	08/04/2021	+	1958670
	100920714	15/04/2021	-	--
	100921989	22/04/2021	+	--
P015	100918099	01/04/2021	+	133778
	100919359	08/04/2021	+	300478
	100920707	15/04/2021	+	--

P129	100918026	01/04/2021	+	515038
	100928558	08/04/2021	+	378824
	100928587	15/04/2021	+	--

Table 5. Results of samples collected from 1st to 23rd of April 2021.

Locator	Identification number	Days analysed	69-70del results	Concentration (GU/L)
P048	100918178	01/04/2021	-	--
	100919462	09/04/2021	+	9975
	100920812	16/04/2021	+	1215101
	100922135	23/04/2021	+	--
P170	100918167	01/04/2021	+	4760012
	100920760	16/04/2021	+	52214
	100922134	23/04/2021	-	--
P150	100918170	01/04/2021	+	51216
	100919481	09/04/2021	+	151003
	100920746	16/04/2021	+	769860
	100922117	23/04/2021	+	--
P070	100918174	01/04/2021	-	--
	100919470	09/04/2021	-	--
	100920820	16/04/2021	+	71741
	100922136	23/04/2021	-	--

Table 6. Results of samples collected from 1st to 13th of April 2021.

Locator	Identification number	Days analysed	69-70del results	Concentration (GU/L)
P006	100917985	01/04/2021	+	17249
	100950364	06/04/2021	-	--
	100919346	08/04/2021	-	--
P008	100917987	01/04/2021	+	15201
	100918517	06/04/2021	-	--
	100919349	08/04/2021	+	538146
	100920026	13/04/2021	-	--
P013	100917998	01/04/2021	+	4418
	100950367	06/04/2021	+	30462
	100950372	08/04/2021	-	--
P014	100951182	01/04/2021	-	--
	100919333	08/04/2021	+	373542
	100950398	13/04/2021	-	--
P019	100918004	01/04/2021	-	--
	100950370	06/04/2021	+	49103
	100950376	08/04/2021	-	--
	100919948	13/04/2021	-	--
P009	100918516	06/04/2021	-	--
	100950381	08/04/2021	+	131221
	100950407	13/04/2021	-	--
P008	100918517	06/04/2021	-	--
	100919349	08/04/2021	+	538146
	100920026	13/04/2021	-	--

P015	100950368	06/04/2021	+	132145
	100919337	08/04/2021	-	--
P017	100950369	06/04/2021	-	--
	100919353	08/04/2021	+	19436
	100919950	13/04/2021	-	--

Table 7. Results of samples collected from 7th to 21st of April 2021.

Locator	Identification number	Days analysed	69-70del results	Concentration (GU/L)
P099	100919162	07/04/2021	+	722717
	100920503	14/04/2021	+	320078
	100921911	21/04/2021	+	--
P079	100919169	07/04/2021	+	917577
	100920510	14/04/2021	+	110096
P078	100919172	07/04/2021	+	124927
	100920466	14/04/2021	+	529708

Table 8. Results of samples collected from 6th to 13st of April 2021.

Locator	Identification number	Days analysed	69-70del results	Concentration (GU/L)
P011	100918513	06/04/2021	+	24332
	100919355	08/04/2021	-	--
	100950403	13/04/2021	-	--
P016	100918676	06/04/2021	-	--
	100950374	08/04/2021	-	--
	100950395	13/04/2021	+	6450122
P010	100950366	06/04/2021	+	55231
	100950380	08/04/2021	+	53796
	100950405	13/04/2021	-	--
P004	100918521	06/04/2021	-	--
	100950384	08/04/2021	+	152067
	100950404	13/04/2021	+	14447

Annex 3. Calculation of RT-qPCR efficiency. Extracted from Svec *et al*. (65).

$$\text{Efficiency} = 10^{(-1/\text{slope})} - 1$$

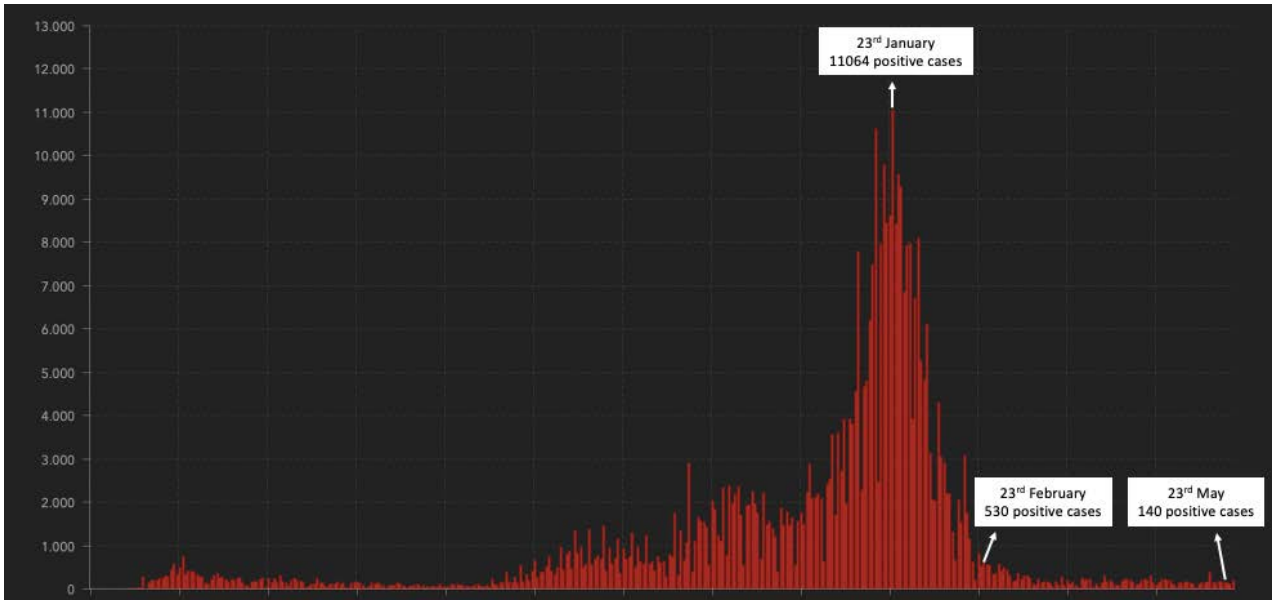

Annex 4. Positive cases in the Valencian Community from 9th March 2020 to 24th May 2021. Y axis represents number of positive cases and x axis represents each day. Positive cases of 23rd January, February and May days are highlighted. Extracted from Generalitat Valenciana datos coronavirus (68).